國立臺灣大學生物資源暨農學院

植物病理與微生物學系

碩士論文

Department of Plant Pathology and Microbiology

College of Bioresources and Agriculture

National Taiwan University

Master Thesis

探討受仙人掌 X 病毒與紅龍果 X 病毒感染影響之寄主基因

Investigation of host genes affected by *Cactus virus X* and *Pitaya virus X* infection

李克

Ke Lee

指導教授：張雅君 博士

林詩舜 博士

Advisor: Ya-Chun Chang, Ph.D.

Shih-Shun Lin, Ph.D.

中華民國一百零九年七月

July 2020

doi:10.6342/NTU202003267

誌謝

花了三年時間，終算走到了這裡。一路走來真的得到很多人的幫助才得以完成這份論文。

首先要感謝的當然是父母。謝謝你們願意給我足夠多的空間，支持我的選擇並給予我各種方面的援助。

謝謝指導老師張雅君教授這三年來的各種幫助，無論是在實驗、課業上的建議還是生活上的關心，都讓我獲益良多。感謝林詩舜教授以及教授實驗室的同學們從零開始手把手教導我從如何建構轉錄體一路到後面的網路分析，沒有大家我恐怕不可能完成這份論文。也謝謝農藝系的劉力瑜教授在百忙之中擠出時間參加我的口試，並給我許多建議。因為有三位老師的指導，我才能從碩班畢業。

當然，我也要感謝 403 實驗室的大家。謝謝沛延學姊、佳君學姊、雅筑學姊、思淮學長、靖益學長、悅民學姊、陳臻學姊、怡樺學姊和岱妤學姊教我做實驗並引導怕生的我融入 403 的環境，也謝謝雅媛、俊耀與采蘋一直以來的互相勉勵與幫助。特別感謝學妹奕秀在實驗上的各種幫忙還有陪我度過種種磨難與試煉，也謝謝學弟孝軒總是找我一起買飯。在 403 的回憶實在太多，無論是岱妤的跌倒還是奕秀的噴嚏，雅媛和俊耀的粉紅泡泡抑或是實驗室的笑聲，都是對我來說極為珍貴的回憶，也許我會這麼帶著他們直到踏進棺材的那一刻吧。總之，一直以來真的都謝謝了。

這邊也想謝謝高師大的王惠亮教授以及實驗室的翁老學長與瑩珊學姊、還有當年一起共患難的蔡明叡啟蒙我對於碩班的興趣。若是沒有諸位，想必我也不會有機會打這篇謝詞了。

最後的最後，我想感謝自大學以來的伴侶怡珊。研究所的旅程雖有歡笑，但淚水占了絕大多數。我絕對無法獨自走完這段崎嶇的荊棘之路。正因為有

doi:10.6342/NTU202003267

妳的陪伴，我才能順利走過這段路。有妳在身邊我感到很幸福。

碩士並非終點，而是另一段故事的開始。期許之後自己能夠帶著大家的祝福繼續往那白色的明天邁進。

doi:10.6342/NTU202003267

中文摘要

仙人掌科三角柱屬(*Hylocereus* spp.)的紅龍果是熱帶地區常見的水果作物。根據報告，目前台灣感染紅龍果的病毒有仙人掌 X 病毒(CVX)、紅龍果 X 病毒(PiVX)和蟹爪蘭 X 病毒(ZyVX)三種。田間調查顯示，在台灣主要紅龍果種植區中紅龍果植株均至少感染這三種 *Potexvirus* 屬病毒中的一種，且常見複合感染。因這些紅龍果病毒的分子感染機制仍待探討，本論文採用轉錄體與文獻搜尋的方法研究紅龍果與這些病毒之間的交互作用。熱休克蛋白 70 家族(Hsp70s)和葉綠體磷酸甘油酸激酶被已被報導為其他 potexvirus 的相關的寄主基因，以這些植物蛋白為對象，分析被 CVX 和 PiVX 感染的植物。半定量反轉錄聚合酶連鎖反應的結果顯示，Hsp70c-4 的表現量在 PiVX 感染的圓葉菸草中被向下調控。至於初步的轉錄體分析，分別以對照組、感染 CVX 和 PiVX 的紅龍果(*H. undatus*)總 RNA 進行次世代定序，利用 de-novo 組裝法，總共獲得 60,510 個片段重疊組(contig)；之後使用阿拉伯芥(TAIR)和歐洲分子生物學實驗室(EMBL)的編碼序列(cds)資料庫，進行註解和開放閱讀框(ORF)預測。透過轉錄體表現量與文獻搜索，自差異表現基因中挑出 11 個主要研究目標。為驗證轉錄體資料的可信度，從中找出 *HSPRO2* 與 *BMY3* 作為參考基因，並以定量 RT-PCR 分析幾個差異表現基因的表現量，但結果與轉錄體資料不符。為了取得更有說服力的結果與資料，對另外兩批紅龍果 RNA 樣品進行定序，並結合之前的定序資料重新建構轉錄體。根據不同處理之間的基因表現量的變化和皮爾森相關係數，建構出基因網絡圖。PiVX 感染網路圖的初步分析揭露數個與離層酸相關的基因被負調控，而參與在吉貝素訊息傳導路徑的基因也發現被調控；暗示 PiVX 感染可能會影響吉貝素訊息傳導路徑，並抑制離層酸訊息傳導路徑。CVX 感染網路圖所包含的基因數量遠高於 PiVX，其中幾個已被報導的 potexvirus 寄主因子與主要目標基

doi:10.6342/NTU202003267

因也在其中，但他們在 CVX 感染中扮演的角色仍待探討。CVX 和 PiVX 感染的紅龍果網絡共享 38 個基因，其中 heat shock transcription factor A2 (*HSFA2.2*)、outer membrane tryptophan-rich sensory protein-related gene (*TSPO*) 和 phytochrome interacting factor 3 (*PIF3*)的基因表現量皆顯著低於對照組，但這些基因對 CVX 與 PiVX 感染的貢獻仍屬未知。總而言之，本研究為我們解析 CVX 和 PiVX 感染如何影響其寄主紅龍果，提供了基礎資料與未來研究方向。

關鍵字：紅龍果、寄主因子、仙人掌 X 病毒、紅龍果 X 病毒、轉錄體分析

doi:10.6342/NTU202003267

Abstract

Pitaya (*Hylocereus* spp.), in the family *Cactaceae*, is a common fruit crop in tropical regions. Three potexviruses, *Cactus virus X* (CVX), *Pitaya virus X* (PiVX), and *Zygocactus virus X* (ZyVX), are reported to infect pitayas in Taiwan. Field surveys revealed that all pitayas at the major planting area of Taiwan are infected by at least one of the three potexviruses and mixed infections are commonly found. Because the molecular infection mechanisms of these potexviruses have not yet been revealed, in this study transcriptome approach and paper mining were applied to investigate the interaction between pitaya and its viruses. Among previously reported host genes related to potexviruses, heat shock protein 70 family and chloroplast phosphoglycerate kinase were selected and used to analyze the CVX and PiVX-infected plants. Semiquantitative RT-PCR revealed that expression level of *Hsp70c-4* was down-regulated in PiVX-infected *Nicotiana benthamiana*. As for preliminary transcriptome analysis, purified total RNAs of mock, CVX- and PiVX-infected pitaya (*H. undatus*) plants were collected for next-generation sequencing. A total of 60,510 contigs were assembled using *de novo* assembly method followed by annotation and open reading frame prediction with TAIR and EMBL cds databases. We eventually selected 11 primary targets from differentially expressed genes (DEGs) based on their expression levels in transcriptome and literature review. To confirm transcriptome results, the expression levels of several DEGs were verified with quantitative RT-PCR using *HSPRO2* and *BMY3* as reference genes which were identified from the transcriptome data. The results of quantitative RT-PCR and transcriptome were different from each other. To obtained a more convincing result, another two sets

doi:10.6342/NTU202003267

of pitaya RNA samples were sequenced to construct a transcriptome combined with previous sequencing data. Gene-to-gene networks were generated based on fold changes between genes in each treatment and their calculated Pearson correlation coefficient value. Early analysis of PiVX infection network disclosed that several ABA-associated genes were down-regulated, while genes involved in GA signaling pathway were also found to be regulated, suggesting that PiVX infection may affect GA signaling pathway and influence ABA signaling pathway. Infection network of CVX contained a lot more genes than that of PiVX, and few reported potexvirus host genes and primary targets were found in the network, but their roles in the infection of CVX required more study. Network of CVX- and PiVX-infected pitayas shared 38 genes. Among them, the expression levels of heat shock transcription factor A2 (*HSFA2.2*), outer membrane tryptophan-rich sensory protein-related gene (*TSPO.2*) and phytochrome interacting factor 3 (*PIF3*) in CVX- and PiVX-infected treatments were significantly lower than mock treatment. Nevertheless, how these genes contribute to the infections of CVX and PiVX remain unclear. In short, this study improves our understanding of how CVX and PiVX infection affect their pitaya host, and provides the basic information and future research direction.

Keywords: pitaya, host factor, *Cactus virus X*, *Pitaya virus X*, transcriptome analysis

doi:10.6342/NTU202003267

Table of content

doi:10.6342/NTU202003267

doi:10.6342/NTU202003267

doi:10.6342/NTU202003267

doi:10.6342/NTU202003267

Introduction

Pitaya and its viral diseases in Taiwan

Pitayas, members of the genus *Hylocereus* in the family *Cactaceae*, are fruit crops distributed in tropical and subtropical regions (CABI, 2020). Based on the mature fruit flesh color, they can be divided into white-fleshed pitayas (*H. undatus*) and red-fleshed pitayas (*H. costaricensis* and *H. polyrhizus*). In recent years, pitayas have drawn the attention of consumers worldwide due to their richness in nutrients (Sonawane, 2017), dietary fiber, antioxidants (Zhuang et al., 2012), and potential curative effect for several modern chronic diseases (Ramli et al., 2016; Song et al., 2016; Guimarães et al., 2017). In agriculture practice, pitayas can be easily grown and maintained, and their fruiting season lasts for months (Bellec et al., 2006). These characteristics of pitaya earn its increasing popularity among farmers and customers over the years. In Taiwan, the planting area of pitaya was 380 hectares in 1999, and that number reached 2754 hectares in 2018 (Council of Agriculture, Executive Yuan, Taiwan).

Common diseases of pitaya are mostly fungal diseases, including stem canker disease caused by *Neoscytalidium dinidiatum* (Chuang et al., 2012), wet rot disease by *Rhizopus stolonifera*, and anthracnose by *Colletotrichum* spp. (Ni et al., 2013). However, pitayas can also be infected by several viruses, which include *Cactus virus X* (CVX), *Pitaya virus X* (PiVX), *Zygocactus virus X* (ZyVX), and *Schlumbergera virus X* (SchVX) (Mao at al., 2018). Among them, three viruses are reported to infect pitaya in Taiwan: CVX, PiVX, and ZyVX. CVX was the first discovered cactus-infecting potexvirus in 1958 (Amelunxen, 1958) and was later found to be wide-spread among *Cactaceae* species. The first

doi:10.6342/NTU202003267

report of CVX-infected pitaya in Taiwan was in 2001 (Liou et al., 2001). PiVX is a novel potexvirus species identified by our lab in 2008 in the samples acquired from Yangmingshan (Mao, 2008). PiVX causes less severe symptoms compared to CVX (Lee, 2010). ZyVX was originally identified as an isolate of CVX (Brandes and Bercks, 1963) but was later classified as a new species of the genus *Potexvirus* based on molecular evidences and host responses (Koenig et al., 2004). Our lab also discovered the presence of ZyVX in samples obtained from Yangmingshan (Mao, 2008). All these viruses belong to the family *Alphaflexiviridae*, the genus *Potexvirus*.

A field study was performed by our lab in 2015 in order to understand the situation of viral infection of pitayas. This investeigation covered the major pitaya planting sites in Taiwan, including Erlin, Wandan, Jiadong, Zhuanwei, and Chishang. The result indicated almost all pitayas are infected by at least one of the three viruses (Guo, 2017). The study demonstrated that mixed infections of these viruses are common in pitaya field, with 20% of all the samples infected by both CVX and PiVX, 59% infected by all three viruses. (Guo, 2017; Huang, 2017). This result highlights the importance of pitaya viral disease and the necessity to solve the problem.

Characteristics of the genus *Potexvirus*

Potexviruses have filamentous virus particles and single-stranded, positive-sense linear RNA genome which contains a methylguanosine cap at 5' end, 5 open reading frames (ORF), and a poly A tail at 3' end (Huisman et al., 1988). It is believed that potexvirus species have no insect vectors and rely solely on mechanical approach for transmission (Koenig and Lesemann, 1978). ORF1 of

doi:10.6342/NTU202003267

potexviruses encodes RNA-dependent RNA polymerase (RdRP), which is responsible for 5' cap biogenesis and the RNA synthesis (Draghici et al., 2009). ORF2 to 4 encode the triple gene block proteins (TGBp1 to 3), which involve in viral movement (Lin et al., 2006). Apart from viral movement, TGBp1 is considered a multifunctional protein. In some species, TGBp1 was shown to participate in several aspects of viral replication and translation (Liou et al., 2000; Kalinina et al., 2002; Rodionova et al., 2003; Lin et al., 2004; Karpova et al., 2006). TGBp1 was also proven to be a silencing suppressor in *Potato virus X* (PVX), the type species of the genus *Potexvirus* (Voinnet et al., 2000). The ORF5 of potexvirus encodes viral coat protein (CP), which involves in viral particle assembly and cell-to-cell movement (Baratova et al., 1992; Rouleau et al., 1995). Other than that, 5'-UTR and 3'-UTR of the viruses are also proposed to have roles in viral infection. On the research of PVX, 5'-UTR was shown to be important for viral replication, genomic RNA accumulation, and cell-to-cell movement (Miller et al. 1998; Kwon and Kim, 2006; Lough et al., 2006). Conserved sequences of PVX and *Bamboo mosaic virus* (BaMV) at 3'-UTR were also reported to regulate the biosynthesis and accumulation of both positive and negative strand viral RNA (Cheng et al. 2001).

In previous study, phylogenetic analyses of CVX, PiVX, and other potexviruses demonstrated that all cactus-infecting potexviruses belong to the same cluster (Mao, 2008). The research showed that CVX and PiVX are actually divided into a different group from other potexviruses, which indicates the enormous research potential within these viruses.

doi:10.6342/NTU202003267

Relationship between viruses and host genes

Since viruses have very limited genome size, they utilize components that can be acquired from their hosts. In fact, viruses rely heavily on their hosts at every aspect of their infection cycles, such as recruiting a series of host factors to assist their organelle targeting, virus replication complex forming, replication, assembly, cell-to-cell movement and systemic movement (Garcia-Ruiz, 2019). Sometimes, a virus would interact with host factors directly for their vital processes, while occasionally the expression of the host genes would be regulated by viral infection to create a preferred condition for viral infection or movement (Garcia-Ruiz, 2019). *Potexvirus* is one of the most well-studied genera and there are numerous reports suggested possible host genes of potexviruses (Table 1). In the case of BaMV, the potexvirus is proposed to grab a ride from chloroplastic phosphoglycereate kinase (chl-PGK) and chloroplastic heat shock protein 70 (cpHsp70) with heat shock protein 90 (Hsp90) escorting the viral replication complex all the way to chloroplast, recruiting glutathione S-transferase tau 4 (GSTU4) along the way, which later helps the replication complex fight against the reactive oxygen species stress in chloroplast (Huang et al., 2012; Chen et al., 2013; Cheng et al., 2013a; Huang et al., 2017). At the same time, 5' to 3'exonuclease (XRN4) assists BaMV by downregulating siRNA-mediated RNA silencing pathway (Lee et al. 2016). For viral movement, RabGTPase-activating protein NbRabGAP1 may participate in cell-to-cell movement and the systemic movement by activating RabGTPases, a protein group involves in vesicle trafficking (Huang et al., 2013). Serine/threonine kinase-like protein and casein kinase 2α (CK2α) will aid the release of viral ribonuclear protein complex through plasmodesmata (Cheng et al., 2013b). In

doi:10.6342/NTU202003267

the case of PVX, the type species of the genus *Potexvirus*, *Tobacco mosaic virus*-movement protein 30-binding protein 2C and DnaJ-like protein (DnaJ) were reported to involved in viral replication (Cho et al., 2012). In addition, remorins, TGB2-intera cting host cellular proteins, β-1,3-Glucanase, SGT1, casein kinases, PVX CP-interacting protein 1, and DnaJ were reported to involve in PVX movement (Park et al., 2013). It is no doubt that host factors play important roles in the infection cycle of viruses, and virus rely heavily on host factors for efficient virus infection and movement. Despite replication and movement, viruses also have to worry about antiviral responses of the host plants, and in most cases components of the viruses would interact with certain host factors to deal with those responses. It is suggested that TGBp1 of PVX interacts with Argonaute 1 (AGO1) protein and mediates the degradation of AGO1 to suppress RNA silencing pathway (Chiu et al., 2010). While AGO1 restricted accumulation of BaMV, it is suggested that BaMV-derived small interfering RNAs could be recruited by AGO10 which in terms increased the replication and accumulation of BaMV (Huang et al., 2019). For efficient replication, viruses must find ways to suppress or bypass the defense system of host plants.

Transcriptome analysis as an approach to investigate potential host factors

When it comes to host factor identification, the most common strategy is to find host proteins that interact with a particular component of virus by means of coimmunopercipitation (coIP) and yeast two hybrid assay (Hsu and Spindler, 2012). At times this would be trouble-making especially if one is dealing with a non-model organism with little or no protein data available. In this case, transcriptome analysis could serve as a promising alternative. Thanks to the

doi:10.6342/NTU202003267

advanced development of sequencing technology, the cost of high-throughput sequencing has dropped to a much more affordable level for laboratories to perform and utilize in various aspects of studies (Jiang et al., 2015). In addition to that, data from transcriptome can be further applied to coIP, microarray, and other assays. The wide-adaptive nature of transcriptome has led to its gaining popularity. By looking into the mRNA expression levels of genes, investigation of differentially expressed genes (DEGs) in different plant treatments have proven to be a solid and reliable mean (Finotello and Camillo, 2015). Lu et al. (2012) attempted to study the systemic symptom development of *Cucumber mosaic virus* by examine the gene expression pattern through transcriptomic approach. Li et al. (2018) performed transcriptome analysis to explore mechanisms of the host plant defense of *Nicotiana benthamiana* (tobacco) against *Tobacco curly shoot virus*. Liu et al. (2014) used network analysis based on the transcriptome data to identify genes with the potential of participating in leafy flower transition mediated by Peanut witches'-broom phytoplasma in *Catharanthus roseus*.

Hypothetically, if a plant gene is important to a virus, it will be reasonable to assume that expression of the gene would be highly possible to be regulated by viral infection. Based on this assumption, we proposed that genes showed different expression levels under viral infection have a great chance being involved in viral infection. Transcriptome analysis provided us a brilliant insight of what genes are up-/down- regulated during viral infection, hence making the screening of potential host genes easier than ever.

doi:10.6342/NTU202003267

Research motive and experimental design

The previous field study performed by our lab revealed that most pitayas in Taiwan were already infected by CVX, PiVX, and ZyVX. Nevertheless, only few publications mentioned these three viruses, and details of the infection of these viruses have yet to be discussed. The aim of this research is to investigate host genes involving in the infection of CVX and PiVX, the most common viruses present in the pitaya field of Taiwan. In this research, we tried to uncover the molecular infection mechanisms of CVX and PiVX by identifying host genes affected by the infection of these viruses. We first did the screening of host genes related to potexviruses through paper mining and transcriptome analysis. Expression levels of potential host genes of CVX and PiVX identified from paper mining under viral infection were further tested. Relation of the DEGs identified from the transcriptome analysis were calculated to generate networks which contain genes that are critical for virus infection.

doi:10.6342/NTU202003267

Materials and methods

Plant cultivation

In this study, plants were grown in 25°C greenhouse. The photoperiod was set 16 h light/ 8 h dark. For tobacco (*Nicotiana benthamiana*), three seeds were planted in each cell of sowing tray filled with filtered peat moss (BVB, Nertherlands) and transferred to 2.5-inch pots filled with 2:1 soil/Gen-Chi-Wan No.3 (Nan Hai Gardencing CO., Taipei, Taiwan) mixture after 7 to 10 days. Jack's Professional 20-20-20 General Purpose Water Soluble Fertilizer (J.R. Peters, Allentown, PA, USA) was given twice per week after plantation, and the plants were watered on daily basis. For pitaya (*Hylocereus undatus*), the seeds were first planted in 3.5-inch pot and the seedlings were transferred to sowing trays in 1:1 soil/Gen-Chi-Wan mixture after 17 to 20 days. The pitaya plants were watered twice per week and no fertilizer was applied.

Agroinfiltration with binary vector clones

The binary vectors, pGB-EV, pGB-CVX, and pGB-PiVX, constructed by previous laboratory members were transformed into *Agrobacterium tumefaciens* C58C1 and stored at -80°C storage in LB with 50% glycerol. The bacteria were streaked onto LA plate containing 50 ppm kanamycin (Kan) and 10 ppm tetracycline (Tet) from -80°C freezer and incubated at 28°C for 2-4 days. Then, several colonies were incubated in 5 ml LB containing 50 ppm Kan at 28°C for 18-24 h with 225-250 rpm. The *A. tumefaciens* cultures were then collected by 2.9 × g centrifugation for 3 minutes and the pellet was resuspended in 1 ml MMA induction buffer (10 mM MES, 10 mM $MgCl_2$, 200 μM acetosyringone).

doi:10.6342/NTU202003267

Concentration of the 100X diluted bacterial suspensions was measured by spectrophotometer (Libra S22 UV/Vis, Biochrom, Cambridge, UK) and adjusted to OD_{600} = 0.5 with MMA buffer. The bacterial suspension was incubated at room temperature (RT) in dark for 1.5-2 h with shaking of 50-75 rpm on Orbital shaker (TS-520, Yihder Co., Taiwan). After induction, the bacterial suspensions were infiltrated into tobacco leaves with 1-ml needleless syringe. The infiltrated leaves were harvest at 2 and 3 days post infiltration (dpi) and stored at -80°C.

Isolation of plant total RNA and removal of DNA

The infiltrated tobacco leaves from at least 2 plants were collected at 2 dpi, weighted and stored at -80°C refrigerator. In this research, total RNA was extracted with Plant Total RNA Mini kit (Viogene, Sunnyvale, CA, USA). Around 0.2 g of leaf samples were first grinded into powder using liquid nitrogen and collected by microcentrifuge tubes. Then, 450 μl RX Buffer was added to the powdered sample and mixed by vortexing before transferred to Shearing tube followed by 16,060 × g centrifugation at 4°C for 2 min. After that, the flow-through sample fluid was mixed with 230 μl 98% ethanol and transferred to plant total RNA mini tube, centrifuged at 4°C for 1 min with 9,500 × g. Next, the samples were washed by 500 μl WF buffer with 16,060 × g centrifugation at 4°C for 1 min and washed twice by 700 μl WS Buffer with 16,060 × g centrifugation at 4°C for 1 min. After that, the samples were centrifuged at 4°C for 3 min with 16,060 × g and air-dried for 2-5 min to remove residual ethanol. The mini columns were then transferred to RNA-free microcentrifuge tube and RNA was eluted by 35-50 μl ddH_2O. Concentration of the RNA samples were quantified by spectrophotometer (NanoDrop™ 1000, ThermoFisher Scientific, Waltham,

doi:10.6342/NTU202003267

MA, USA).

After RNA extraction, DNA removal was then performed using TURBO DNA-free™ Kit (Invitrogen, Thermo Scientific, ThermoFisher Scientific). Ten micrograms of total RNA were added into a 50 μl reaction solution with 1X TURBO DNase™ Buffer and 2U TURBO DNase™ Enzyme. The samples were incubated at 37°C for 1 h. Six microliters DNase Inactivation Reagent were added followingly and incubated at room temperature for 5 min with constant flicking to avoid precipitation. The samples were centrifuged at 10,000 × g for 90 sec and the RNA supernatants were transferred to new RNA-free microcentrifuge tubes and quantified by NanoDrop.

Detection of Cactus virus X and Pitaya virus X by multiplex RT-PCR

Multiplex RT-PCR developed by Mao (2008) was used to detect the infection of *Cactus virus X* and *Pitaya virus X*. At first, 6 μl total RNA was mixed with 2 μl 5 μM mt-R3 primer, 1 μl 5 μM CVX-R5 primer,1 μl 5 μM PiVX-R8 primer, and 1 μl 5 μM ZyVX-R9 primer and incubated at 65°C for 12 minutes. The samples were put on ice for 5 minutes followed by the addition of 2.5 μl 5X AMV RT Buffer, 1.25 μl 10 mM dNTPs (Promega, Madison, USA), 0.25 μl rRNasin (40 U/μl, Promega), and 0.25 μl AMV RT (10 U/μl, Promega). The samples were briefly spun and incubated at 42°C for 1 hour for reverse transcription, and then followed by termination at 70°C for 10 min. After that, 2 μl RT product was used in each 20 μl reaction with PCR master mix containing 1X TnATaq buffer, 0.25 μM mt-F2/R3 primers, 0.025 μM CVX-F5/R5 primers, 0.025 μM PiVX-F6/R8 primers, 0.025 μM ZyVX-F9/R9 primers, 0.2 mM dNTPs, and 0.75 U TnATaq polymerase (BIOTnABiotech, Kaoshiung, Taiwan).

doi:10.6342/NTU202003267

The PCR program was set as 95°C for 5 min as denaturation, followed by 30 cycles of 95°C for 30 sec, 56°C for 30 sec, and 72°C for 1 min and 30 sec. The extra extension step was set 72°C for 7 min followed by 4°C for 5 min cooldown. Gel electrophoresis was performed with 1.5% agarose gel at 135 voltage and stained with EtBr.

Detection of CVX and PiVX by western blot

For western blot, 0.1-0.3 g of leaves were grinded to powder and mixed with 2X volumes of GUS extraction buffer (10 mM EDTA, 0.1% SDS, 50 mM sodium phosphate, 0.1% Triton X-100, 10 mM β-mercaptoethanol, and 1 mM PMSF). The solutions were collected by microcentrifuge tubes and centrifuged at 4°C for 10 minutes with 13680 × g. Supernatant was mixed with 2X sample buffer (4% SDS, 20% glycerol, 25 mM EDTA, 0.04% bromophenol blue and 0.1 M Tris HCl, pH 6.8, 4% β-mercaptoethanol) and loaded into 10% SDS-polyacrylamide gel for electrophoresis. After that, proteins were electrotransferred to Immobilon^{R}-P Transfer Membrane (Merk, Burlington, MA, USA). The membrane was blocked with 5% skimmed milk at 37°C for 45 min and then incubated with 10000X diluted anti-PiVX-CP antibody prepared with 1% skimmed milk at 37°C for 45 min, washed by PBS-T buffer (137 mM NaCl, 2.7 mM KCL, 10 mM Na_2HPO_4, 1.8 mM KH_2PO_4, 0.05% Tween-20, pH 7.4) for 3 times (10 min each). Then the membrane was again incubated with 20000X diluted ECL^{TM} Anti-rabbit IgG-HRP (in 1% skimmed milk) at 37°C for 45 min followed by washing. After that, the membrane was put into a plastic bag and incubated with appropriate volume of Immobilon Western Chemiluminescent HRP Substrate (Merck) for detection. The results were visualized by

doi:10.6342/NTU202003267

photographic film. The membrane was further stained with Coomassie Brilliant Blue R-250 solution (0.15% Coomassie Brilliant Blue R-250, 45% methanol, 10% acetic acid) which served as protein loading control.

Semiquantitative RT-PCR

Reverse transcription was performed with Superscript™ III Reverse Trasnscriptase (Invitrogen). Each 13 μl reaction contained 1,000 ng total RNA, 1 μl 50 μM dTVN primer, and 1 μl 10 mM dNTPs. The samples were incubated at 65°C for 5 minutes and put on ice for at least 2 minutes. After that, 4 μl 5X First Strand Buffer, 1 μl 0.1 M DTT, 1 μl rRNasin (40 U/μl), and 1 μl Superscript™ III RT (200 U/μl) were added. The reactions were incubated at 50-55°C for 1 h and then followed by 70°C for 15 minutes to terminate the reaction. The samples were further diluted 2-3 times to perform the following procedures.

For semi-quantitative PCR, each 20 μl reaction contained 2 μl cDNA, 1X Taq DNA Polymerase Master Mix RED, 1 μM forward primer, 1 μM reverse primer. Different PCR programs were set for different target genes. The PCR program was set 95°C for 5 min as denaturation, and extra extension step was set 72°C for 7 min followed by 4°C for 5 min cooldown. The cycle number, annealing temperature, and extension time were set depends on the amplified target. For heat shock protein 70 cytoplasmic isoform 1 (*Hsp70c-1*), rubisco small subunit (*RbcS*) and chloroplastic phosphoglycerate kinase (*chl-PGK*), the program was set 95°C for 30 sec, 55°C for 30 sec, and 72°C for 48 sec with the cycle number of 25. Electrophoresis was run at 135V with 1% gel, and samples were loaded 2 μl for Hsp70c-1 and RbcS, and 3 μl for chl-PGK, respectively. For Hsp70 endoplasmic reticulum isoform 1 (*Hsp70er-1*) and Hsp70

doi:10.6342/NTU202003267

chloroplastic isoform 1 (*Hsp70cp-1*), the program was set 95°C for 30 sec, 43°C for 30 sec, and 72°C for 48 sec with the cycle number of 30. Electrophoresis was run at 135V with 1% gel, and 7 μl of samples was loaded into each well. For Hsp70c-4, the program was set 9°5C for 30 sec, 50°C for 30 sec, and 72°C for 24 sec with the cycle number of 25. Electrophoresis was run at 135V with 2% gel, and 5 μl of samples was loaded into each well.

Virus inoculation, RNA isolation and RNA sequencing

Healthy, CVX, PiVX-infected *Chenopodium quinoa* leaves were weighed and grinded in 10 volumes of inoculation buffer (0.1 M sodium phosphate, pH 7.4) for mechanical inoculation. Ten microliters of healthy and virus-infected plant saps were separately inoculated on each cotyledon of 21-day-old pitayas with the help of carborundum. The cotyledons were harvested at 17 dpi pair by pair (each pair was around 0.1-0.2 g). The extraction of RNA was performed with Plant Total RNA Mini kit as described above except using different buffer. In this case, 450-500 μl PRX Buffer was added to the powdered pitaya sample and mixed by vortexing before transferred to Shearing tube. The rest of the procedure remained the same. Six to eight pitaya RNA samples of each treatment (mock, CVX, and PiVX) with the best condition regarding 260/280 value and nucleic acid concentration were mixed together and viral infection was confirmed by multiplex RT-PCR. After that, 6G throughput sequencing was performed using Hi-seq 4000 for the first sample set and Nova seq 6000 machine for the second and third sample sets (Genomics BioSci & Tech Co., Taiwan). The read quality was examined using MultiQC (version 1.2). Low quality bases and sequencing adapters in the raw data were removed using Trimmomatic

doi:10.6342/NTU202003267

(version 0.38) to generate clean data.

***De novo* assembly**

For preliminary transcriptome construction, clean data of the first sample set, which includes mock, CVX-, and PiVX-infected treatments, was used for *De novo* assembly with CLC Genomics workbench Version 7.5.1 (QIAGEN, CLC bio, Hilden, Germany). The parameters were set as word size 30, bubble size 60, and the rests remained default. The assembled contigs were annotated to their best-matched coding sequence (cds) using BLAST with TAIR10 and EMBL database (). The reads of different treatments were then mapped to the assembled contigs using bowtie2 (http://bowtie-bio.sourceforge.net/bowtie2/index.shtml), and the read counts of each contig in each treatment were later normalized as fragments per kilobase million (FPKM) using deepseq2 (https://bioconductor.org/packages/release/bioc/html/DESeq2.html). In order to determine differentially expressed genes (DEGs), expression levels of the contigs in different treatments were compared based on their FPKM. For full transcriptome construction, all the clean data from 3 sets of mock, CVX-, and PiVX-infected treatments were used for *De novo* assembly with the sample protocol.

Differentially expressed gene identification and gene-to-gene network analysis

In preliminary transcriptome, differentially expressed genes (DEGs) were defined as complete genes that show at least 2 times fold change in FPKM between mock treatment and virus-infected treatment.

doi:10.6342/NTU202003267

In full transcriptome, DEGs were identified using the network function (version 3) in the ContigViews system (http://www.contigviews.bioagri.ntu.edu.tw/) with parameters set as complete and partial genes that showed at least 3-fold differences with 60% passing rate for the repeats. Relation between these identified DEGs were then calculated using Pearson correlation cofefficient (r) and genes with high correlation (0.9 for positive and -0.85 for negative) were presented as a network. In the network, each circle represents a gene and the lines connecting the circle indicates the correlation between the genes.

Validation of the expression level of potential host genes related to CVX and PiVX with quantitative RT-PCR

For the primer design of quantitative PCR (qPCR), Genscript Real-time PCR (TaqMan) Primer design tool (https://www.genscript.com/tools/real-time-pcr-taqman-primer-design-tool) and AmplifX (version 1.7) were used. Coding sequence of the target genes were given to the Genscript design tool with the parameters set at 20 primer sets, 100-200 PCR amplicon size, default primer T_m and default probe T_m. The organism parameter was set to others. Quality of the generated primer pairs would then be checked by AmplifX. Those with the best quality were selected as the primers for qPCR assay. Specificity of the primer pair was checked by regular RT-PCR before the primers were used in qRT-PCR.

The protocol of RNA extraction was the same as previously described, and several RNA samples were mixed to reduce individual variation. After RNA isolation, TURBO DNA-free^{TM} Kit (Invitrogen) was applied to remove residual DNA in the RNA samples. The procedure was almost the same as previously described except a few modifications. In this case, 44 μl of total RNA was mixed

doi:10.6342/NTU202003267

with 5 μl 5X TURBO DNase™ Buffer and 1 μl TURBO DNase™ Enzyme (2 U/μl). The samples were incubated at 37°C for 1 h. Six microliters of DNase Inactivation Reagent were added followingly and incubated at room temperature for 5 min with constant flicking. The samples were centrifuged at 10,000 × g for 90 sec and the RNA supernatant were transferred to new RNA-free microcentrifuge tubes and quantified by NanoDrop.

After DNA removal, reverse transcription was performed with Superscript™ III Reverse Transcriptase (Invitrogen). Each 13 μl reaction contained 200-300 ng total RNA, 1 μl 50 μM dTVN primer, and 1 μl 10 mM dNTPs. The samples were incubated at 65°C for 5 minutes and put on ice for at least 2 minutes. After that, 4 ml 5X First Strand Buffer, 1 μl 0.1 M DTT, 1 μl rRNasin (40 U/μl), and 1 μl Superscript™ III RT (200 U/μl) were added. The reactions were incubated at 50-55°C for 1 h followed by 70°C for 15 minutes to terminate the reaction. Afterwards, the samples were further diluted 2 times.

For qPCR reaction, each sample contained 1 μl of the diluted cDNA, 1X SYBR Green Master Mix (Applied Biosystems, Waltham, Massachusetts, USA), 0.5 μM forward primer, and 0.5 μM reverse primer. Each treatment had three repeats. qPCR was performed with Applied Biosystem machine using advanced set up with conditions set as 96 wells/SYBR Green reagent/ΔΔCt/Standard and with program setting as follows: 95°C for 10 minutes, 40 cycle of 95°C for 15 seconds and 60°C for 1 minutes. Cycle threshold of each treatment given by the machine was calculated manually to ΔΔCt values using *HSPRO2* or *BMY3* as internal control pitaya gene.

doi:10.6342/NTU202003267

Results

Examination of heat shock protein 70s and chl-PGK as potential host genes of CVX and PiVX

1. Heat shock protein 70s and chloroplast phosphoglycerate kinase are selected as potential host genes due to similarity between CVX and other potexviruses

In order to find potential host genes involved in the replication and accumulation of CVX and PiVX, we reviewed previously reported host genes related to potexviruses (Table 1). From the literatures, we found that Hsp70s can be linked to the infection of *Potato virus X* (PVX), *Pepino mosaic virus* (PepMV), and *Bamboo mosaic virus* (BaMV), and infection of these viruses induced at least 1 member of Hsp70s (Chen et al., 2008; Mathioudakis et al., 2014; Huang et al., 2017). With this finding, it seemed quite promising that CVX and PiVX could upregulate the expression levels of Hsp70s and utilize some of them as host factors. Consequently, Hsp70s were selected as potential host genes for the following assays. In the study of BaMV, which was observed to replicate in chloroplasts (Lin and Chen, 1991), cpHsp70s assist viral chloroplast-targeting. Since CVX was also observed to replicate in chloroplasts (Chen and Tzeng, 1996), we expected that CVX infection would upregulate cpHsp70s. Another chloroplast-related protein, chloroplastic phosphoglycerate kinase (chl-PGK), was also reported to be involved in the chloroplast-targeting of BaMV. Here we proposed that since CVX and BaMV replicate in chloroplasts, the chances are high that both viruses would exploit similar host genes, and picked chl-PGK as another potential host genes and expected it to be upregulated by CVX. Since

doi:10.6342/NTU202003267

CVX and PiVX are closely related, we believed that CVX and PiVX have similar infection strategies and therefore expected the infection of both CVX and PiVX would induce cpHsp70s and chl-PGK.

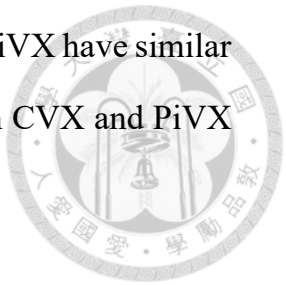

2. CVX or PiVX infection did not induce the expression of *Hsp70cp-1* and *chl-PGK*, but downregulated *Hsp70c-4*

Previously, a study revealed that PVX infection induced expression of a series of Hsp70s, and the investigation included various isoforms of Hsp70s (Chen et al., 2008). Here we examined the expression levels of those Hsp70s plus chl-PGK under CVX or PiVX infection. Since tobacco is not a natural host of CVX and PiVX, the viruses are not able to move from cell to cell and viral infection is restricted at unicellular level. To overcome this obstacle, binary vector clones of CVX and PiVX, pGB-CVX and pGB-PiVX, were agroinfiltrated into 4 to 5-week-old tobacco plants. Accumulation of the viruses were tested via westernblot, and the infection could be detected as early as 2 dpi (Fig. 1A). Multiplex RT-PCR was also performed to confirm viral infection and whether there were contaminations between the tobacco plants. The result also confirmed viral RNA accumulation at 2 dpi (Fig. 1B), indicating by 2 dpi both CVX and PiVX have successfully infected tobacco leaves without contamination.

To study the expression levels of Hsp70s and chl-PGK under viral infection, the binary vectors were agroinfiltrated into the 7th, 6th, 5th true leaves of tobacco followed by semiquantitative RT-PCR (semi-qRT-PCR) at 2 dpi. Expression levels of the tested genes resulted in very different patterns regarding different experiments (data not shown). However, the quantified data of semi-qRT-PCR revealed that at 2 dpi, expression levels of cytoplasmic Hsp70-4 (*Hsp70c-4)* were

doi:10.6342/NTU202003267

significantly decreased in PiVX-infected tobacco across all tested leaves, whereas the expression levels of other Hsp70s and chl-PGK in PiVX-infected leaves did not show significant difference from those of empty vector-infiltrated tobacco (Fig. 2). As to CVX-infected leaves, *Hsp70c-4* and chl-PGK were significantly downregulated only at the 6th leave (Fig. 2). The results indicated that PiVX infection downregulates *Hsp70c-4* but not other heat shock proteins and chl-PGK, while in CVX infection Hsp70c-4 and chl-PGK were significant downregulation only at 6th tobacco leaves but not at other tested leaves.

Preliminary transcriptome analysis

1. Transcriptome construction

To further investigate possible host genes of CVX and PiVX in their natural host, transcriptome analysis of pitaya was performed (Fig. 3). In preliminary transcriptome construction, total RNAs of mock, CVX- and PiVX-infected pitayas were extracted from the inoculated cotyledons at 17 dpi and multiplex RT-PCR was performed to confirm viral infection and exclude the possibility of contamination (Fig. 4). After that, the pitaya RNA samples were sequenced. At this point, each treatment had only one sample with no repeats. RNA-sequencing generated 190,142,562 reads in total including 65,997,124 mock reads, 58,861,704 CVX reads, and 65,283,734 PiVX reads (Table 2). Since there was no available reference genome data for pitaya, these pair-end reads were used for *de novo* assembly to construct pitaya transcriptome. *De novo* assembly of all reads from mock, CVX, and PiVX treatment generated a total of 60,510 contigs (Table 2). The assembled contigs were named after PTY (eg. PTY1, PTY2, and so forth). After annotation and ORF prediction by BLASTx using TAIR and

doi:10.6342/NTU202003267

EMBL cds databases as describe in the work of Liu et al. (2014), 9,557 contigs (16% of all) were classified as complete contigs (have both start and stop codons and good alignment rate), 10,744 contigs (18%) were classified as partial (lacks start or stop codons but has good alignment rate), and 40,209 contigs (66%) were grouped to undefined contigs (No hit in BLAST or lacks start or stop codons and gas bad alignment rates) based on the method described in the work of Liu et al. as well (Table 2).

Next, to investigate the sequence similarities between model organism Arabidopsis and pitaya, complete contigs of pitaya and their best-matched Arabidopsis coding sequences were compared. Length distributions of the amino acid sequence of pitaya showed similar patterns to Arabidopsis (Fig. 5), and most of the average amino acid identity is approximately 30-45% (Fig. 5). Lengths of the matched protein sequences between these two plant species are highly correlated as the correlation coefficient is above 0.9 (Fig. 7). Although the amino acid sequence identities are between 30-45%, similar sequence length in protein sequences and their high correlation suggests that annotation of the complete pitaya contigs using Arabidopsis data is a proper mean.

2. Selection of pitaya primary targets

To further determine genes that are significantly affected by CVX and PiVX infection, a set of conditions were used to filter the genes. Since at this stage we only obtained one set of data in each treatment, a rough approach was implemented to identify differentially expressed genes (DEGs) and primary targets for further research by using a series of fold change conditions. DEGs were first identified as complete contigs with fold change ≥ 1.5 or ≤ 0.67. During

doi:10.6342/NTU202003267

this step, data of CVX was found to be extremely low at both counts and FPKM value (data not shown). Because of the lack of repeats, we suspected that there might have some abnormal complications in the CVX treatment and therefore CVX was excluded from the DEG identification process. For that reason, the identification process was performed with the data from mock and PiVX only. After the process, 3737 genes were identified as DEGs (Fig. 8). It was surprising that all the remaining DEGs were downregulated in PiVX-infected pitayas. To further reduce numbers of the remaining candidates, strict parameters, which FPKM should be above 100 in at least one treatment and fold change ≥ 2 or ≤ 0.5, were applied. The resulting 364 DEGs were further filtered with the condition that at least FPKM should be above 850 in one treatment, and the remaining 38 DEGs were designated potential host genes (Fig. 8).

Through data mining, reports of these potential host genes were studied in details. Eleven of them have been previously linked to virus infections and were therefore selected as primary targets (Table 3). Among the primary targets, most of the genes are related to photosynthesis and photosystems, including light-harvesting chlorophyll-protein complex I subunit A4 (*LHCA4*), photosystem I light harvesting complex gene 3 (*LHCA3*), photosystem I subunit G (*PSAG*), photosystem I subunit K (*PSAK*), photosystem II subunit O-2 (*PSBO2*), and plastocyanin 1 (*PETE1*). This result suggested that PiVX infection could potentially alter chloroplast metabolism and affect photosynthesis, which supports our speculation that chloroplasts may be the replication site of PiVX.

doi:10.6342/NTU202003267

3. Attempts to validate few potential primary targets reveal the potential of *HSPRO2* as a reference gene of qRT-PCR while the results were contradicted to the transcriptome data

In order to validate the transcriptome data, qRT-CR was performed. A reference gene that shows similar and stable expression level across all samples is needed for qRT-PCR in order to compare the relative expression levels of the genes of interest. In usual cases, actin and elongation factor-1α are two common genes to be considered as reference genes for qPCR (Kozera and Rapacz, 2013). However, in our preliminary transcriptome data, FPKM values of these two genes were five times lower in PiVX-infected pitayas compared to mock treatment (Fig. 9A and B). Consequently, a search of alternative reference genes was conducted. In the query, we found two genes, Ortholog of sugar beet HS1 PRO1-2 (*HSPRO2*) and β-amylase 3 (*BMY3*), have similar FPKM values between mock and PiVX-treated pitayas (Fig. 9C and D). Although there were no literatures that used *HSPRO2* and *BMY3* as reference genes, both genes showed similar expression between treatments at the transcription level so as to be considered as potential pitaya reference genes. To validate the expression pattern of preliminary transcriptome data, we picked a few DEGs as tested genes, and two sets of pitaya samples were tested with both *HSPRO2* and *BMY3* as reference genes. In the case of *BMY3*, expression patterns of the genes showed great variation between two samples, with only *PETE1* showed similar expression pattern of mock, CVX, and PiVX treatments between the samples (Fig. 10A and B). In the case of *HSPRO2*, only one gene, *DI21*, showed different expression levels between CVX and PiVX (Fig.10C and D). These results suggested that *HSPRO2* would potentially be a better internal control than *BMY3*.

doi:10.6342/NTU202003267

However, the results of qRT-PCR are contradicted to our transcriptome data that all the DEGs were downregulated by PiVX infection, as most of the genes were upregulated by the infection of PiVX according to the qRT-PCR results. When looked at the fold change axis of the figures, it is clear that the fold change of the first test is dramatically 2-3 times higher than the second test (Fig. 10C and D). This could potentially indicate that the expression level of *HSPRO2* is not stable, which diminished its possibility of being a reference gene for qRT-PCR of CVX- and PiVX-infected pitayas.

Full transcriptome analysis

1. Construction of transcriptome

After the preliminary transcriptome construction, another two sets of samples were sent for RNA-sequencing. All three repeats of pair-end reads were used to construct a new transcriptome (Fig. 11). RNA-sequencing generated 610,601,596 reads in total including 197,056,782 mock reads, 204,483,750 CVX reads, and 209,061,064 PiVX reads (Table 4). *De novo* assembly using reads from all three repeats of mock, CVX-, and PiVX-treated pitayas generated 80,875 contigs, which includes 8,949 complete genes (11.07%), 13,397 partial contigs (16.57%), and 58,529 undefined contigs (Table 4). The assembled contigs were named start with PTYV3. When comparing proteins from the best-matched complete coding sequences between Arabidopsis and pitaya, length distributions of the pitaya amino acid sequence showed similar patterns to Arabidopsis the reference (Fig. 12), and average amino acid identity is around 25-45% (Fig. 13). Lengths of the matched protein sequences between the two plant species are highly correlated as the correlation coefficient value suggests

doi:10.6342/NTU202003267

(Fig. 14). Although identity of the protein amino acids was slightly lower than the previous transcriptome construction, the results again suggested that annotation of the complete pitaya contigs using Arabidopsis data is a proper mean.

2. Expression levels of potential potexvirus host genes and previously identified primary targets in the full transcriptome

After the construction of transcriptome, we used BLAST to find the best-matched proteins of known potexvirus host genes and then checked the expression levels of these potential host genes in pitaya. While counterparts of some reported host genes could not be found in full transcriptome, some sequences matched to the same contig using BLAST, such as *Hsp70c-1* and *Hsp70-4* all matched to *HuHsp70.2* (Fig. S1). All the potential host genes pulled out showed decreased expression in CVX-infected pitayas (Fig. 15). Some potential host genes showed no or little different expression levels in PiVX-infected treatment, such as *HuATG10a, HuATG8f, HuHsc70, HuHsp70c.1, HuHsp70c.2, HuHsp70er,* and *HuXRN4*. Some genes were downregulated in the infection of both viruses, which includes *HuCK2α, HucpHsp70, HuPETE1*, *HuPsbO.1*, *HuRAGB3f*, and *HuTIP*. Two genes, *HuHsp70c.2* and *HuHsp90*, were upregulated by PiVX infection (Fig. 15). It is interesting that in paper mining step host genes of potexviruses were mostly found to be upregulated during viral infection, but in the transcriptome data most of these pitaya genes were downregulated by viral infection, which is the exact opposite.

The expression levels of primary targets selected in preliminary transcriptome were also checked in the full transcriptome. All primary targets

doi:10.6342/NTU202003267

were downregulated in both CVX and PiVX-infected pitayas (Fig.16), which are the same as in preliminary transcriptome. It was obvious that CVX and PiVX share some regulation preferences but still they adopted slightly different strategies to accomplish successful infection.

3. Gene-to-gene network of PiVX-infected treatments revealed ABA and GA signaling pathways may participate in PiVX infection

In the preliminary transcriptome analysis, a rough method was used to identify potential host genes which were based solely on FPKM values. Now the transcriptome was constructed with three sets of samples, strategy with more credibility could be applied to identify genes that are critical to virus infection. To understand which DEGs are important to virus infection, gene-to gene-network was constructed for PiVX-infected pitayas. First, DEGs were identified by the condition set 60% passing rate and 3 times fold change. After that, Pearson correlation coefficients (r) between two genes were calculated, and genes with high correlation were picked up and presented in the network ($r \geq 0.9$ or ≤ -0.85). In the network, genes are displayed as dots and the link between the dots indicates their relation (red as the positive and green as the negative). Genes in the network were grouped to different classes based on literatures. In the network of PiVX, ninety genes were divided to several groups based on their functions in stress and relations with phytohormones: general stress-related genes (involved in stress/resistance response but not reported to be regulated by phytohormones), chloroplast-related genes, ROS-related genes, ABA-related genes, other hormone-related genes (genes regulated by one hormone), multiple hormone-related genes (genes regulated by more than one hormones), and non-classified

doi:10.6342/NTU202003267

genes (Fig.17). We checked the network for potential potexvirus host genes and primary targets, and none of them were in the network. Most genes in this network showed positive relation between each other. Only a few genes showed negative relationship between each other, which includes *ATAF1.2*/*ANAC2*, *HIA3*, *AHG3/PP2CA*, *RD26*/*ANAC72*, *AITR2/DIG1*, *SWEET13/PRG2*, *HB7*, and *EXP15* (Fig. 18A). Among them, most genes were downregulated by PiVX infection, only *EXP15* was upregulated (Fig. 19A). Most of these genes are grouped to be associated with ABA, suggesting that ABA signaling may play a role in the infection of PiVX, but the roles of ABA signaling in PiVX infection remains to be further investigated. *EXP15* is a cell wall-loosening agent (Wieczorek et al., 2006), upregulation of the gene could potentially help cell-to-cell and systemic movement of the virus. The network linked *EXP15* to several ABA-associated genes, implying that the gene might be regulated by ABA pathway. *SWEET13/RPG2* is the only gene to show solely negative relation to other genes (Fig. 18A), and the gene was proposed to be involved in GA response (Kanno et al., 2016). The information combined indicated that both ABA and GA signaling pathways might be crucial to PiVX infection.

In the PiVX infection network, three genes were isolated from other genes and only showed positive correlation with each other (Fig. 18B). These genes are FAR1-related sequence 11 (*FRS11*), Histone 1.2 (*H1.2*), and lipase 1 (*LIP1*). All three genes are upregulated by PiVX infection (Fig. 19B). H1.2 is a linker histone which involves in transcriptional activation and repression (Rea et al., 2012), and FRS11 is a nuclear protein which is important for phytochrome A (phyA)-mediated far-red light responses (Lin et al, 2004), and LIP1 is a TAG lipase involved in GA signaling (Rombolá-Caldentey et al, 2014). Through their

doi:10.6342/NTU202003267

functions, it seems logical to assume that upregulation of *H1.2* would affect the expression of *FSR11* and *LIP1*, which in terms enhance phytochrome A-mediated far-red light responses and GA signaling. However, whether and how these pathways contribute to PiVX infection required further investigation.

4. Gene-to-gene network of CVX-infected treatments shared a few genes with PiVX

In order to compare infection transcriptome of CVX and PiVX, gene-to-gene network of CVX was generated with the same conditions as PiVX network. As mentioned previously, the network of PiVX only contains 90 genes. In the case of CVX, however, there are over 1200 genes in the initial network, suggesting that CVX infection may cause more transcriptional changes than that of PiVX. We also checked the CVX network for both potential potexvirus host genes and primary targets, and three of them were presented in the network. These three genes include plastocyanin (*PETE1*), photoglycerate kinase (*PGK*), and transcriptionally-controlled tumor protein (*TCTP*) (data not shown). Networks between the treatments of CVX and PiVX shared 38 genes (Table 5), and three of them are in the top 10 genes with most connections in PiVX infection network, which includes heat shock transcription factor A2 (*HSFA2.2*), outer membrane tryptophan-rich sensory protein-related gene (*TSPO.2*), and phytochrome interacting factor 3 (*PIF3*). HSFA2.2 is considered to be involved in heat stress memory (Ohama et al., 2017). TSPO is a membrane protein mostly found in epidermis and can be induced by ABA (Guillaumot et al., 2009). PIF3 is a transcription factor that interacts with phytochrome A and phytochrome B and it is a possible negative regulator of phyB-mediated processes (Pham et al., 2018).

doi:10.6342/NTU202003267

HSFA2.2, *TSPO* and *PIF3* were all downregulated by CVX and PiVX infection (Fig. 19B), but their pathological meaning remained to be determined. The size of CVX infection network is too large and therefore the analysis has not been finished.

doi:10.6342/NTU202003267

Discussion

Function of Hsp70s and Chl-PGK in virus infection

Hsp70s are molecular chaperones which assist proper protein folding and prevent protein degradation (Mayer and Bukau, 2005). The family has been reported to relate to infection of numerous viruses. In *Potexvirus* alone, PVX infection upregulates several Hsp70s of tobacco (Chen et al., 2008), NbcpHsp70-2 has been proven to be important to BaMV infection (Huang et al., 2017); while tobacco Hsp70c interacts with the coat protein of PepMV and is proposed to facilitate viral replication (Mathioudakis et al., 2014). Besides potexviruses, Hsp70 is required for the infection of *Tomato yellow leaf curl virus* (Gorovits et al., 2013), replication of *Red clover necrotic mosaic virus* (Mine et al., 2012) and *Beet black scorch virus* (Wang et al., 2018). Hsp70 is also involved in viral particle disassembly of *Cucumber necrosis virus* (Alam and Rochon, 2017). It is evident that Hsp70s can be utilized by viruses across different realms.

In this study, expression levels of several Hsp70 isoforms mentioned by Chen (2008) were tested. Although all Hsp70s didn't show any consistent regulation patterns in CVX-infiltrated tobacco plants, PiVX infection was observed to downregulate *Hsp70c-4* expression (Fig. 2). It should be noted that in this study, *Hsp70c-2* and *Hsp70c-3* could not be amplified from all available treatments using primer pairs published by previous studies (data not shown). It is interesting that PiVX only regulates *Hsp70c-4* but not another isoform *Hsp70c-1* (Fig. 2). One of the reasons could be the variation of the full-length sequence between *Hsp70c-1* and *Hsp70c-4* leads to different binding targets that would jeopardize PiVX infection or promote the degradation of PiVX

doi:10.6342/NTU202003267

components. It could also be the case that Hsp70c-4 would compete the binding targets of PiVX proteins, hence create the need to suppress its expression. In BaMV infection, cpHsp70s are involved in chloroplast targeting of the virus and are upregulated by viral infection (Huang et al., 2017). However, this might not be the case for CVX and PiVX as the infection didn't induce their expression, and two hypotheses may be able to explain the observed outcome. In the study of BaMV, overexpression of potential host factors would not necessarily lead to increased accumulation or replication of viruses as the expression levels of the potential host factors might be sufficient for viral replication already (Cheng et al., 2013; Huang et al., 2017). We proposed a similar scenario that in this case the viruses did not induce the expression of tested genes because the original expression level is sufficient enough for successful infection. However, Hsp70s are known to be induced by various stress conditions (Mayer and Bukau, 2005), which makes the scenario a little bit unlikely. Indeed, another possibility is that CVX and PiVX simply adopt different strategies and do not exploit same set of host factors as BaMV and PVX, and therefore there are no needs to regulate those genes.

Chl-PGK, a chloroplastic isoform of PGK, is a protein participates in glucometabolism (Banks et al., 1979). Discussion of its roles in virus infection was next to none. However, it was reported that chl-PGK assists the organelle targeting of BaMV (Chen et al., 2013). Since CVX and PiVX are similar to BaMV in terms of their possible replication sites in chloroplasts, we proposed that both viruses could exploit similar host components as BaMV. In this study, we did not observe significant and similar expression pattern of *chl-PGK* by CVX and PiVX infection. Like we previously discussed, it is possible that we

doi:10.6342/NTU202003267

never observed the changes because the expression level of *chl-PGK* is already sufficient enough for infection of CVX and PiVX or CVX and PiVX do not utilize chl-PGK as a host factor.

It should be noted that at 6th leaves of tobacco, *Hsp70c-4* and *chl-PGK* also showed significant down-regulation in CVX-infiltrated leaves (Fig. 2). However, we argue that an important host gene should show universal viral regulation pattern among all tested leaves regardless of their positions, considering the fact that the viral infection can be detected in all virus-infiltrated leaves. If a host gene is truly essential to the virus, it should be utilized by the virus in every case. The fact that down-regulation of *Hsp70c-4* and *chl-PGK* could only be observed at 6th leaves but not the other 2 tested leaves positions (5th and 7th) indicated that down-regulation might be due to other factors rather than CVX infection.

Different viral regulation of Hsp70s between tobacco and pitaya

In previous discussions, we mentioned that *Hsp70c-1* and *Hsp70c-4*, two partial Hsp70 genes in tobacco, matched to the same pitaya contig, *Hsp70c.2* (PTYV3_1546), in full transcriptome (Fig. S1). In our test in tobacco, PiVX infection downregulates *Hsp70c-4* but not *Hsp70c-1* (Fig. 2). However, in the full transcriptome, *Hsp70c.2* was upregulated during the infection of PiVX. It is obvious that PiVX infection seemed to have different regulation on Hsp70s between tobacco and pitaya. Here we argue that tobacco and pitaya are very different species and tobacco is not even the natural host of PiVX. It is highly possible that PiVX utilizes different set of host genes and regulates certain host genes differently in order to accomplish successful infection in these two plant species. The hypothesis of course remains to be further proven.

doi:10.6342/NTU202003267

Low RNA extraction efficiency of pitaya

In this study, one of the most challenging part is the extraction of pitaya total RNA. Purification of pitaya RNA using Plant Total Extraction kit with optimized protocol usually results in RNA concentration between 10-80 ng/μl, which is extremely low for regular reverse transcription practice and far from the requirement for RNA-sequencing. The idea of mixing multiple RNA samples into one is not only to reduce individual variation but to meet the concentration standard for sequencing. Other commercial extraction kits have been tested but did not show much differences in final RNA concentration (data not shown). The reason why RNA elution step in pitaya samples is different from that of tobacco is exactly due to the low concentration nature of purified total RNA samples. It would be extremely beneficial for us to develop an efficient RNA extraction protocol of pitaya.

Construction and validation of preliminary transcriptome

For preliminary pitaya transcriptome, we constructed a transcriptome based on the first set of sequencing data and tried to reduce the number of potential host genes in order to select primary targets by comparing their FPKM values and fold change between the treatments. A total of 38 DEGs with highest FPKM values and biggest fold change were reviewed. The result ended up with 11 primary targets which have been reported to be involved in viral infection. It is perhaps not surprising that these primary targets are mostly related to chloroplasts, as previous studies have linked viral infection to the alteration of chloroplasts (Dardick, 2007; Havelda et al., 2008). In our cases, however, we believe that CVX and PiVX replicate in chloroplasts, so it makes perfect sense

doi:10.6342/NTU202003267

for CVX and PiVX to regulate the expression of proteins related to chloroplasts for efficient infection. We did not examine the function of these targets since they were selected based on merely one set of samples and more repeats were needed to verify the results. However, we did try to validate some of them by checking the transcriptome data. At first we intended to use common reference genes as internal control. However, in the prelimirary transcriptome, FPKM of actin and *EF1α* showed huge fold changes between mock and PiVX-infected treatment (Fig. 9A and B). Consequently, we reviewed other possible candidates in the preliminary transcriptome, and found *BMY3* and *HSPRO2* to be promising candidates (Fig. 9C and D). Nevertheless, RT-qPCR results showed that both genes may not be the best candidate for reference genes under viral infection (Fig. 10). Recently, Chen et al. (2019) have examined the credibility of a series of common reference genes in pitaya (*H. undatus*). In their study, actin and *EF1a* are actually the most stable gene across different developmental stages and temperature stress. During literature review, we did find that *EF1α* is a potexvirus host gene (Table 1). Therefore, we believe *EF1α* may not be a proper choice for reference gene in our case. We check the expression levels of popular reference genes discussed by Chen (2019) and Kozera (2013), but all of them seemed to be regulated by viral infection in transcriptome, with alpha tubulin (*TUBA*) showed least differences between different treatments (Fig. S2). Previous laboratory study has proven that *PP2A* is a proper reference gene for tobacco under PiVX infection and *β*-actin to *Chenopodium quinoa* under viral infection, respectively (Chang, 2017; Huang, 2017). These results suggest that acceptable reference genes differ between plant species and under viral infections. In order to find the legitimate reference gene for pitaya, potential

doi:10.6342/NTU202003267

common reference genes should still be tested regardless of their expression patterns in the transcriptome data, and other genes show similar expression levels should be tested as well. At the end of the day, genes showed similar cycle threshold value should be able to serve as reference genes for qPCR of pitaya under CVX and PiVX infection.

Full transcriptome highlights different expression pattern between CVX, PiVX, and other potexviruses

A second attempt of transcriptome construction using a total of three sets of mock, CVX-, and PiVX-infected pitayas was later performed. The expression levels of previously reported potexvirus host genes and primary targets were checked. A different expression pattern of genes was observed as some identified potexvirus host genes were not regulated by infection of CVX and PiVX while some even showed opposite regulation. This indicates that although in the same genus, infection mechanism within a viral genus could still differ from Each other. Whether the opposite expression pattern contributes to viral infection remains further investigation. Previous study has classified CVX and PiVX to a distinct group of potexviruses (Mao, 2008), but even CVX and PiVX seemed to have different strategies for successful infection as they showed dissimilar expression pattern (Fig. 15 and 16). In most cases of the potential host genes and primary targets we picked up, CVX showed significant differences not only to mock but to PiVX, clearly indicates that the two viruses have different effects on pitaya gene expression. Synergetic interaction between CVX and PiVX has previously been studied (Wu, 2019). As synergism usually works with two organisms that adopt different survival strategies, the different expression pattern

doi:10.6342/NTU202003267

between CVX and PiVX infection could provide evidences and insights of the synergism between CVX and PiVX.

In preliminary transcriptome, we observed considerably low values of count and FPKM in CVX treatment but failed to conclude the reason. In full transcriptome, we can still observe the relative low values in CVX treatment. Since we have a total of 3 sets of samples in the full transcriptome, we believe these results are the genuine status in CVX-infected pitayas rather than unexpected errors in sequencing.

Large proportion of unidentified genes in the transcriptomes

In both transcriptome constructions, a large proportion of assembled contigs were not identified (Table 2 and Table 4). In this study, we only used the information acquired from TAIR and EMBL databases. There are only few transcriptomic data of the *Cactaceae* family, and most of them were available as raw sequencing data rather than databases for reference (Hua et al, 2016; Song et al., 2016; Xu et al, 2019). The undefined genes could be novel genes within the genus and the family which have yet to be discovered and studied. That means we have very little information about those genes, and hence we did not analyze the undefined genes in this study. However, these genes contain huge research potential and should be further investigated.

Network analysis revealed that PiVX infection may influence GA signaling pathway and inhibit ABA signaling pathway

In this study, we constructed a gene-to-gene network of PiVX based on the FPKM fold change between mock and PiVX-infected treatment. The resulting

doi:10.6342/NTU202003267

network includes 90 genes, and most of them were positively related to each other (Fig. 17). In addition, most genes in the network were downregulated by PiVX infection (data not shown). In the network, some of the genes stood out as they showed negative connections to other genes. Most of these genes could be linked with ABA, and two of them, *AHG3/PP2CA* and *AITR2*/*DIG1*, were previously identified as negative regulators of ABA signaling (Yoshida et al., 2006; Tian et al., 2017). Considering that the expression levels of these genes were both downregulated in transcriptome analysis (Fig. 19), it is reasonable to propose that these two genes act downstream of other ABA-associated genes and possibly function as negative feedback in ABA signaling. *ATAF1.2/ANAC2* is a NAC (No Apical Meristem) domain transcription factor known to be involved in various responses, including plant development and stress responses (Liu et al., 2016). This gene and its isoform both have fair amount of connections to other genes, suggesting they may be a crucial player in the infection of PiVX. In the infection of *Tobacco mosaic virus*, *ATAF2* is one of the genes to be upregulated as host defense responses (Wang et al., 2009). *ATAF1* is also reported to be involved in biotic stress, so we suspected *ATAF1* may be downregulated due to its role in plant defense. *HB7*, *HIA3*, and *RD26/ANAC72* are reported to be involved in stress response (Söderman et al., 1996; Huang et al., 2007; Chung et al., 2014), and the fact that they are all positively related to *ATAF1.2/ANAC2* suggested that they may be regulated by *ATAF1.2/ANAC2*. *EXP15* is reported to function in cell wall-loosening (Wieczorek et al., 2006), and the network shows that *EXP15* is negatively related to the ABA-associated genes mentioned above (Fig. 18A), which indicates that ABA signaling pathway could possibly repress the expression of *EXP15*. Since EXP15 contains the

doi:10.6342/NTU202003267

function to restructure cell wall, we proposed that PiVX may exploit the role of EXP15 to promote cell-to-cell movement by inhibiting ABA signaling pathway, but the hypothesis needs to be further confirmed. In the network, *SWEET13/RPG2* displayed only negative relation to other genes (Fig. 18A). *SWEET13/RPG2*, a gene involved in modulating GA response (Kanno et al., 2016), has previously been reported to contribute to the susceptibility of bacterial blight caused by *Xanthomonas oryzae* pv. *oryzae* (Oliva et al., 2019). In our case however, *SWEET13/RPG2* was downregulated by PiVX infection, suggesting it plays a different role in PiVX infection. A contradicted result was observed as although negatively related to ABA-associated genes which were downregulated by PiVX infection, the expression of *SWEET/RPG2* was also slightly downregulated by virus infection. At the moment we still cannot explain the observation.

In the PiVX infection network, there are three genes only showed positive connection with each other (Fig. 18B). Among them, H1.2 is responsible for activation and repression of genes, the correlation suggests that the expression of *FSR11* and *LIP1* are highly possible to be regulated by H1.2. Limited research was performed on FSR11, but LIP1 on the other hand is identified as a player in GA signaling. Expression of *LIP1* was clearly upregulated by PiVX infection, but *SWEET13/RPG2*, another GA-related gene previously discussed, was downregulated by PiVX infection. We proposed that LIP1 acts upstream of *SWEET13/RPG2* in GA signaling pathway, but we cannot explain the conflicted results we observed.

In this study, we tried to find connection of the genes presented in the network. Despite our best effort, we couldn't find any solid evidences from the

doi:10.6342/NTU202003267

previous studies to connect these genes. It should also be noted that there are only few upregulated pitaya genes in the network, which is unusual as virus infection usually upregulate a series of host genes (Li et al., 2018). These results indicate that more efforts should be put into the network analysis as the relation of these pitaya genes have not been discussed before in the literatures.

Potential potexvirus host genes and primary targets presented in the CVX infected network

In attempt to understand the lying mechanism under CVX infection, we constructed gene-to-gene network of CVX-infected treatment as well. In order to make the network comparable to that of PiVX, we constructed the CVX network using same parameters as PiVX and resulted in a network contains 1200 genes. Due to limited time scale, we were not able to review all the genes in the network and the attempt to analyze this network was abandoned. Instead, we turned to checked whether the potential potexvirus host genes, primary targets, and genes in PiVX infection network were presented in this infection network of CVX. We then found *PETE1*, a gene on the list of both potential potexvirus host genes and primary targets, was presented in the network. Although *PETE1* is related to the symptom severity and accumulation of PVX, type species of the genus *Potexvirus*, in tobacco chloroplasts, report has asserted that PVX infection did not alter the expression of *PETE1*. In our case, expression *PETE1* is significantly decreased in CVX-infected treatment (Fig. 16), suggesting *PETE1* could play a different role in CVX infection. PGK is a glycolytic enzyme functions in the Calvin cycle, and it has also been reported to participate in multiple virus infection. The protein was observed to be a positive host gene for

doi:10.6342/NTU202003267

infection of *Tomato bushy stunt virus* and *Sugarcane mosaic virus* (Chen et al., 2017; Prasanth et al., 2017), but shown to be downregulated by infection of *Tobacco mosaic virus* (TMV) and *Rice stripe virus* (Bi et al., 2019; Lu et al., 2019). TCTP is a multifunctional protein conserved in the eukaryotes and has been reported to involve in the infection of several viruses. On Arabidopsis, TMV infection increased relative expression of *TCTP* (Gupta et al., 2013). On tomato, *Pepper yellow mosaic virus* infection upregulated *TCTP* (Alfenas-Zerbini et al., 2009). In other cases, TCTP was required for infection of *Potato virus Y* (Guo et al., 2017). Although the functions of these genes in viral infection has been discussed, viruses are known to take different strategies for efficient infection, hence we argue that potexviruses may adopt similar or different infection strategies. All in all, we found PETE1, PGK, and TCTP could be crucial to CVX infection, but their roles in the infection of CVX required further studies.

Common genes presented in both CVX and PiVX networks

Among the 90 genes presented in PiVX infection network, 38 of them are also presented in the 1200-gene CVX infection network (Table 5). Among them, three genes were picked up due to their high connections to other genes in PiVX infection network. While HSFA2.2 seems to be a heat stress response regulator, TSPO are reported to be induced by various stress (Guillaumot et al., 2009). PIF3 are proposed to be a negative regulator of phyB-mediated process (Pham et al., 2018), but how these three genes contribute to the infection of both CVX and PiVX required further query.

doi:10.6342/NTU202003267

Conclusions and Future works

In this study, we tried to investigate potential host genes of CVX and PiVX by data mining and transcription analysis. In the paper mining and further examination, we found that *Hsp70c-4* of *N. benthamiana* was downregulated by PiVX infection. In transcriptome analysis, we constructed pitaya transcriptome through *de novo* assembly approaches and performed network analysis. But before the networks were constructed, we tried to validate the FPKM data of preliminary transcriptome using 2 potential reference genes and failed. Although left unfinished, the current progress suggests that PiVX infection might influence GA signaling pathway and inhibit ABA signaling pathway. In previous studies, CVX was observed to replicate and accumulate faster than PiVX in pitaya, *C. quinoa*, and tobacco (Huang, 2017; Lin, 2017). In this study, we constructed the infection networks of both viruses, and the results showed that CVX infection regulates considerably more host genes then that of PiVX, which may explain the quick infection and obvious symptoms of CVX in pitaya. These results only give us a sneak peek in the mechanism of the infection of CVX and PiVX, further studies need to be performed to discuss the transcriptome data obtained in depth. It is worth noting that in field mixed infection of CVX and PiVX seemed to be more common than single infection. This study has proven that CVX and PiVX regulate different sets of genes during their infection. It is important and essential to further study how mixed infection regulates the host genes to facilitate the infection of both viruses. It should also be noted that in Taiwan red-fleshed pitayas are more popular than white-fleshed pitayas, the species we used in this study. Although two groups of pitayas are closely related to each other, whether the knowledge acquired from white-flesh pitayas can be applied to red-flesh

doi:10.6342/NTU202003267

pitayas remain to be further researched. All things considered, this study shed some light for our understanding of pitayas and paved the way for future studies. More studies are needed to uncover the complicated mechanisms of the infection of CVX and PiVX.

doi:10.6342/NTU202003267

References

Abbink, T. E., Peart, J. R., Mos, T. N., Baulcombe, D. C., Bol, J. F., and Linthorst, H. J. 2002. Silencing of a gene encoding a protein component of the oxygen-evolving complex of photosystem II enhances virus replication in plants. Virology. 295: 307–319.

Alam, S. B. and Rochon, D. A. 2017. Evidence that Hsc70 is associated with *Cucumber necrosis virus* particles and plays a role in particle disassembly. J Virol. 91: e01555-16.

Alfenas-Zerbini, P., Maia, I. G., Fávaro, R. D., Cascardo, J. C., Brommonschenkel, S. H., and Zerbini, F. M. 2009. Genome-wide analysis of differentially expressed genes during the early stages of tomato infection by a potyvirus. Mol Plant Microbe Interact. 22: 352-361.

Amelunxen, F. 1958. Die Virus-Eiwei\spindeln der Kakteen. Darstellung, elektronenmikroskopische und biochemische Analyse des Virus. Protoplasma. 49: 140–178.

Banks, R. D., Blake, C. C., Evans, P. R., Haser, R., Rice, D. W., Hardy, G. W., Merrett, M., and Phillips, A. W. 1979. Sequence, structure and activity of phosphoglycerate kinase: a possible hinge-bending enzyme. Nature 279: 773–777.

Baratova, L. A., Grebenshchikov, N. I., Shishkov, A. V., Kashirin, I. A., Radavsky, J. L., Jarvekulg, L., and Saarma, M. 1992. The topography of the surface of *Potato virus X*: tritium planigraphy and immunological analysis. J. Gen. Virol. 73: 229-235.

doi:10.6342/NTU202003267

Bi, J. A., Yang, Y., Chen, B., Zhao, J., Chen, Z., Song, B., Chen, J., and Yan, F. 2019. Retardation of the Calvin cycle contributes to the reduced CO_2 assimilation ability of rice stripe virus-infected *N. benthamiana* and suppresses viral infection. Front Microbiol. 10: 568.

Brandes, J., and Bercks, R. 1963. Untersuchungen zur Identifizierung und Klassifizierung des Kakteen-X-Virus (cactus virus X). J. Phytopathol. 46:291–300.

Chang,Y.-W. 2017. Study of two *Cactus virus X* infectious clones and establishment of pitaya protoplast system. National Taiwan University. Master thesis.

Chen, C., Wu, J., Hua, Q., Tel-Zur, N., Xie, F., Zhang, Z., Chen, J., Zhang, R., Hu, G., Zhao, J., and Qin, Y. 2019. Identification of reliable reference genes for quantitative real-time PCR normalization in pitaya. Plant methods. 15:70.

Chen, H., Cao, Y., Li, Y., Xia, Z., Xie, J., Carr, J. P., Wu, B., Fan, Z., and Zhou, T. 2017. Identification of differentially regulated maize proteins conditioning *Sugarcane mosaic virus* systemic infection. New Phytol. 215: 1156-1172.

Chen, I. H., Chiu, M. H., Cheng, S. F., Hsu, Y. H., and Tsai, C. H. 2013. The glutathione transferase of *Nicotiana benthamiana* NbGSTU 4 plays a role in regulating the early replication of *Bamboo mosaic virus*. New Phytol. 199:749-757.

Chen, M. J., and Tzeng, D. D.-S. 1996. Identification of cactus X potexvirus in Taiwan and localization of its existence and multiplication in infected cells. Plant Pathol. Bull. 5:63-67.

doi:10.6342/NTU202003267

Chen, Z. R., Zhou T., Wu, X. H., Hong, Y. G., Fan, Z. F., and Li, H. F. 2008. Influence of cytoplasmic heat shock protein 70 on viral infection of *Nicotiana benthamiana*. Mol. Plant Pathol. 9:809-817.

Cheng, J. H., Ding, M. P., Hsu, Y. H., and Tsai, C. H. 2001. The partial purified RNA-dependent RNA polymerases from Bamboo mosaic potexvirus and Potato virus X infected plants containing the template-dependent activities. Virus Res. 80:41-52.

Cheng, S. F., Huang, Y. P., Chen, L. H., Hsu, Y. H., and Tsai, C. H. 2013a. Chloroplast phosphoglycerate kinase is involved in the targeting of *Bamboo mosaic virus* to chloroplasts in *Nicotiana benthamiana* plants. Plant Physiol. 163:1598-1608.

Cheng, S.-F., Tsai, M.-S., Huang, C.-L., Huang, Y.-P., Chen, I-H., Lin, N.-S., Hsu, Y.-H., Tsai, C.-H., and Cheng, C.-P. 2013b. Ser/Thr kinase-like protein of *Nicotiana benthamiana* is involved in the cell-to-cell movement of Bamboo mosaic virus. PLoS One. 8(4): e62907.

Cho, S. Y., Cho, W. K., Sohn, S. H., and Kim, K. H. 2012. Interaction of the host protein NbDnaJ with *Potato virus X* minus-strand stem-loop 1 RNA and capsid protein affects viral replication and movement. Biochem Biophys Res Commun. 417:451-456.

Chiu, M. H., Chen, I. H., Baulcombe, D. C., and Tsai, C. H. 2010. The silencing suppressor P25 of *Potato virus X* interacts with Argonaute1 and mediates its degradation through the proteasome pathway. Mol Plant Pathol. 11:641-649.

Chung, Y., Kwon, S. I., and Choe, S. 2014. Antagonistic regulation of Arabidopsis growth by brassinosteroids and abiotic stresses. Mol Cells. 37:

doi:10.6342/NTU202003267

795-803.

Dardick, C. 2007. Comparative expression profiling of *Nicotiana benthamiana* leaves systemically infected with three fruit tree viruses. MPMI. 20:1004-1017.

Draghici, H. K., Pilot, R., Thiel, H., and Varrelmann, M. 2009. Functional mapping of PVX RNA-dependent RNA-replicase using pentapeptide scanning mutagenesis-identification of regions essential for replication and subgenomic RNA amplification. Virus Res. 143:114-124.

Finotello, F. and Di Camillo, B. 2015. Measuring differential gene expression with RNA-seq: challenges and strategies for data analysis. Brief Funct Genomics. 14:130-142.

Fridborg, I., Grainger, J., Page, A., Coleman, M., Findlay, K., and Angell, S. 2003. TIP, a novel host factor linking callose degradation with the cell-to-cell movement of *Potato virus X*. MPMI. 16(2): 132-140.

Garcia-Ruiz, H. 2019. Host factors against plant viruses. Mol Plant Pathol. 20:1588-1601.

Gorovits, R., Moshe, A., Ghanim, M., and Czosnek, H. 2013. Recruitment of the host plant heat shock protein 70 by *Tomato yellow leaf curl virus* coat protein is required for virus infection. PloS one. 8: e70280.

Guillaumot, D., Guillon, S., Déplanque, T., Vanhee, C., Gumy, C., Masquelier, D., Morsommem P., and Batoko, H. 2009. The Arabidopsis TSPO-related protein is a stress and abscisic acid-regulated, endoplasmic reticulum–Golgi-localized membrane protein. Plant J. 60: 242-256.

doi:10.6342/NTU202003267

Guimarães, D. D. A. B., De Castro, D. D. S. B., Oliveira, F. L. D., Nogueira, E. M., Silva, M. A. M. D., and Teodoro, A. J. 2017. Pitaya extracts induce growth inhibition and proapoptotic effects on human cell lines of breast cancer via downregulation of estrogen receptor gene expression. Oxid Med Cell Longev. 2017:7865073

Guo, S.-M. 2017. Interactions between *Cymbidium mosaic virus* and *Odontoglossum ringspot virus* in *Nicotiana benthamiana*. Department of Plant pathology and Microbiology. National Taiwan University. Master thesis.

Guo, Y., Jia, M. A., Yang, Y., Zhan, L., Cheng, X., Cai, J., Zhang J., Yang, J., Liu, T., Fu, Q., Zhao, J., and Shamsi, I. H. 2017. Integrated analysis of tobacco miRNA and mRNA expression profiles under PVY infection provids insight into tobacco-PVY interactions. Sci Rep. 7: 4895

Gupta, M., Yoshioka, H., Ohnishi, K., Mizumoto, H., Hikichi, Y., and Kiba, A. 2013. A translationally controlled tumor protein negatively regulates the hypersensitive response in *Nicotiana benthamiana*. Plant Cell Physiol. 54: 1403-1414.

Havelda, Z., Várallyay, É., Válóczi, A., and Burgyán, J. 2008. Plant virus infection-induced persistent host gene downregulation in systemically infected leaves. Plant J. 55: 278-288.

Hsu, T. H. and Spindler, K. R. 2012. Identifying host factors that regulate viral infection. PLoS Pathog. 8: e1002772.

Hung, C.-J., Huang, Y.-W., Liou, M.-R., Lee, Y.-C., Lin, N.-S., Meng, M., Tsai, C.-H., Hu, C.-C., and Hsu, Y.-H. 2014. Phosphorylation of coat protein by protein kinase CK2 regulates cell-to-cell movement of *Bamboo mosaic*

doi:10.6342/NTU202003267

virus through modulating RNA binding. MPMI. 27:1211–1225.

Hua, Q., Chen, C., Chen, Z., Chen, P., Ma, Y., Wu, Y., Zheng, J., Hu, G., Zhao, J., and Qin, Y. 2016. Transcriptomic analysis reveals key genes related to betalain biosynthesis in pulp coloration of *Hylocereus polyrhizus*. Front Plant Sci. 6:1179.

Huang, C.-Y. 2017. Investigation of the interaction between *Cactus virus X* and *Pitaya virus X*. Department of Plant pathology and Microbiology. National Taiwan University. Master thesis.

Huang, D., Jaradat, M. R., Wu, W., Ambrose, S. J., Ross, A. R., Abrams, S. R., and Cutler, A. J. 2007. Structural analogs of ABA reveal novel features of ABA perception and signaling in Arabidopsis. Plant J. 50: 414-428.

Huang, Y.-P., Chen, I.-H., and Tsai, C.-H. 2017. Host Factors in the Infection Cycle of *Bamboo mosaic virus*. Front. Microbiol. 8:437

Huang, Y. P., Chen, J. S., Hsu, Y. H., and Tsai, C. H. 2013. A putative Rab-GTPase activation protein from *Nicotiana benthamiana* is important for *Bamboo mosaic virus* intercellular movement. Virology 447, 292–299

Huang, Y.-P., Jhuo, J.-H., Tsai, M.-S., Tsai, C.-H., Chen, H.-C., Lin, N.-S., et al. 2015. NbRABG3f, a member of Rab GTPase, is involved in *Bamboo mosaic virus* infection in *Nicotiana benthamiana*. Molecular Plant Pathology. 17:714–726.

Huang, Y. W., Hu, C. C., Liou, M. R., Chang, B. Y., Tsai, C. H., Meng, M., et al. 2012. Hsp90 interacts specifically with viral RNA and differentially regulates replication initiation of *Bamboo mosaic virus* and associated satellite RNA. PLoS Pathogens. 8

doi:10.6342/NTU202003267

Huang, Y. W., Hu, C. C., Tsai, C. H., Lin, N. S., and Hsu, Y. H. 2017. Chloroplast Hsp70 isoform is required for age-dependent tissue preference of *Bamboo mosaic virus* in mature *Nicotiana benthamiana* leaves. MPMI. 30:631-645.

Huang, Y. W., Hu, C. C., Tsai, C. H., Lin, N. S., and Hsu, Y. H. 2019. *Nicotiana benthamiana* Argonaute10 plays a pro-viral role in *Bamboo mosaic virus* infection. New Phytol. 224:804-817.

Huisman, M. J., Linthorst, H. J., Bol, J. F., and Cornelissen, B. J. 1988. The complete nucleotide sequence of *Potato virus X* and its homologies at the amino acid level with various plus-stranded RNA viruses. J Gen Virol. 69:1789-1798.

Jang, C., Seo, E.-Y., Nam, J., Bae, H., Gim, Y. G., Kim, H. G., Cho, I. S., Lee, Z.-W., Bauchan, G. R., Hammond, J., and Lim, H.-S. 2013. Insights into *Alternanthera mosaic virus* TGB3 functions: Interactions with *Nicotiana benthamiana* PsbO correlate with chloroplast vesiculation and veinal necrosis caused by TGB3 over-expression. Frontiers in Plant Science. 4.

Jiang, Z., Zhou, X., Li, R., Michal, J. J., Zhang, S., Dodson, M. V., Zhang, Z., and Harland, R. M. 2015. Whole transcriptome analysis with sequencing: methods, challenges and potential solutions. Cell Mol Life Sci. 72:3425-3439.

Kalinina, N. O., Rakitina, D. V., Solovyev, A. G., Schiemann, J., and Morozov, S. Y. 2002. RNA helicase activity of the plant virus movement proteins encoded by the first gene of the triple gene block. Virology 296:321-329.

Kanno, Y., Oikawa, T., Chiba, Y., Ishimaru, Y., Shimizu, T., Sano, N., Koshiba, T., Kamiya, Y., Ueda, M., and Seo, M. 2016. AtSWEET13 and

doi:10.6342/NTU202003267

AtSWEET14 regulate gibberellin-mediated physiological processes. Nat Commun. 7: 13245.

Karpova, O. V., Zayakina, O. V., Arkhipenko, M. V., Sheval, E. V., Kiselyova, O. I., Poljakov, V. Y., Yaminsky, I. V., Rodionova, N. P., and Atabekov, J. G. 2006. *Potato virus X* RNA-mediated assembly of single-tailed ternary 'coat protein-RNA-movement protein' complexes. J. Gen. Virol. 87:2731-2740.

Koenig, R., and Lesemann, D.-E. (1978). Potexvirus group. Commonwealth Mycological Institute/Association of Applied Biologists (CMI/AAB) Descriptions of Plant Viruses, 200.

Koenig, R., Pleij, C. W., Loss, S., Burgermeister, W., Aust, H., and Schiemann, J. 2004. Molecular characterisation of potexviruses isolated from three different genera in the family *Cactaceae*. Arch. Virol. 149:903-914.

Kwon, S. J., and Kim, K. H. 2006. The SL1 stem-loop structure at the 5'-end of *Potato virus X* RNA is required for efficient binding to host proteins and for viral infectivity. Mol. Cells. 21:63-75.

Kozera, B. and Rapacz, M. 2013. Reference genes in real-time PCR. J Appl Genet. 54:391-406.

Le Bellec, F., Vaillant, F., and Imbert, E. 2006. Pitahaya (*Hylocereus* spp.): a new fruit crop, a market with a future. Fruits, 61:237-250.

Lee, C.-C., Lin, T.-L., Lin, J.-W., Han, Y.-T., Huang, Y.-T., Hsu, Y.-H., and Meng, M. 2016. Promotion of *Bamboo mosaic virus* accumulation in *Nicotiana benthamiana* by 5' → 3' exonuclease NbXRN4. Front. Microbiol. 6:1508.

doi:10.6342/NTU202003267

Li, K., Wu, G., Li, M., Ma, M., Du, J., Sun, M., Sun, X., and Qing, L. 2018. Transcriptome analysis of *Nicotiana benthamiana* infected by T*obacco curly shoot virus*. Virol. J. 15:138.

Li, K., Wu, G., Li, M., Ma, M., Du, J., Sun, M., Sun, X., and Qing, L. 2018. Transcriptome analysis of *Nicotiana benthamiana* infected by *Tobacco curly shoot virus*. Virol J. 15: 138.

Li, Y.-S. 2010. Characterization, infectious clone construction and antiserum preparation of *Pitaya virus X*. Department of Plant pathology and Microbiology. National Taiwan University. Master thesis.

Lin, M. K., Chang, B. Y., Liao, J. T., Lin, N. S., and Hsu, Y. H. 2004. Arg-16 and Arg-21 in the N-terminal region of the triple-gene-block protein 1 of *Bamboo mosaic virus* are essential for virus movement. J. Gen. Virol. 85:251-259.

Lin, N. S., and Chen, C. C. 1991. Association of *bamboo mosaic virus* (BoMV) and BoMV-specific electron-dense crystalline bodies with chloroplasts. Phytopathology 81:1551-1555.

Lin, P.-Y. 2017. Infection and distribution of *Cactus virus X* and *Pitaya virus X* in pitaya plants. National Taiwan University. Master thesis.

Lin, R. and Wang, H. 2004. Arabidopsis FHY3/FAR1 gene family and distinct roles of its members in light control of Arabidopsis development. Plant Physiol. 136: 4010-4022.

Liou, M. K., Hu, C. C., Lin, N. S., Chang, B. Y., and Hsu, Y. H. 2006. Movement of potexviruses requires species-specific interactions among the cognate triple gene block proteins, as revealed by a trans-complementation assay based on the *Bamboo mosaic virus* satellite RNA-mediated expression

doi:10.6342/NTU202003267

system. J. Gen. Virol. 87:1357-1367.

Liou, D. Y., Hsu, Y. H., Wung, C. H., Wang, W. H., Lin, N. S., and Chang, B. Y. 2000. Functional analyses and identification of two arginine residues essential to the ATP-utilizing activity of the triple gene block protein 1 of Bamboo mosaic potexvirus. Virology 277:336-344.

Liou, M. R., Chen, Y. R., and Liou, R. F. 2001. First report of *Cactus virus X* on *Hylocereus undatus* (*Cactaceae*) in Taiwan. Plant Dis. 85:229.

Liu, L.-Y. D., Tseng, H.-I., Lin, C.-P., Lin, Y.-Y., Huang, Y.-H., Huang, C.-K., Chang, T.-H., and Lin, S.-S. 2014. High-throughput transcriptome analysis of the leafy flower transition of *Catharanthus roseus* induced by peanut witches'-broom phytoplasma infection. Plant Cell Physiol. 55:942–957.

Liu, Y., Sun, J., and Wu, Y. 2016. Arabidopsis ATAF1 enhances the tolerance to salt stress and ABA in transgenic rice. J Plant Res. 129: 955-962.

Lough, T. J., Lee, R. H., Emerson, S. J., Forster, R. L., and Lucas, W. J. 2006. Functional analysis of the 5' untranslated region of potexvirus RNA reveals a role in viral replication and cell-to-cell movement. Virology 351:455-465.

Lu, J., Du, Z.-X., Kong, J., Chen, L.-N., Qiu, Y.-H., Li, G.-F., Meng, X.-H., and Zhu, S.-F. 2012. Transcriptome analysis of *Nicotiana tabacum* infected by *Cucumber mosaic virus* during systemic symptom development. PLoS. ONE. 7: e43447

Lu, Z. S., Chen, Q. S., Zheng, Q. X., Shen, J. J., Luo, Z. P., Fan, K., Xu, S.-H., Shen, Q., and Liu, P.-P. 2019. Proteomic and phosphoproteomic analysis in *Tobacco mosaic virus*-infected tobacco (*Nicotiana tabacum*). Biomolecule. 9: 39.

doi:10.6342/NTU202003267

Mao, C.-H. 2008. Molecular Characterization and Detection of New *Zygocactus virus X* and *Pitaya virus X* from pitaya. Department of Plant pathology and Microbiology. National Taiwan University. Master thesis.

Mao, C. H., Lu, Y. C., Li, Y. S., Chang, Y. C., and Kuo, T. Y. 2018. Pitaya viral diseases and their detection methods in TAIWAN. Management of Pest and Disease. 303.

Mathioudakis, M. M., Rodríguez-Moreno, L., Sempere, R. N., Aranda, M. A., and Livieratos, I. 2014. Multifaceted capsid proteins: Multiple interactions suggest multiple roles for *Pepino mosaic virus* capsid protein. MPMI. 27:1356–1369

Mayer, M. P. and Bukau, B. 2005. Hsp70 chaperones: cellular functions and molecular mechanism. Cell Mol Life Sci. 62:670-684.

Miller, E. D., Plante, C. A., Kim, K. H., Brown, J. W., and Hemenway, C. 1998. Stem-loop structure in the 5' region of *Potato virus X* genome required for plus-strand RNA accumulation. J. Mol. Biol. 284:591-608.

Mine, A., Hyodo, K., Tajima, Y., Kusumanegara, K., Taniguchi, T., Kaido, M., Mise, K., Taniguchi, H., and Okuno, T. 2012. Differential roles of Hsp70 and Hsp90 in the assembly of the replicase complex of a positive-strand RNA plant virus. J Virol. 86:12091-12104.

Ni, H. F., Huang, C. W., Hsu, S. L., Lai, S. Y., and Yang, H. R. 2013. Pathogen characterization and fungicide screening of stem canker of pitaya. J. Taiwan Agric. Res. 62:225–234.

Ohama, N., Sato, H., Shinozaki, K., and Yamaguchi-Shinozaki, K. 2017. Transcriptional regulatory network of plant heat stress response. Trends Plant Sci. 22: 53-65.

doi:10.6342/NTU202003267

Oliva, R., Ji, C., Atienza-Grande, G., Huguet-Tapia, J. C., Perez-Quintero, A., Li, T., Eom, J.-S., Li, C., Nguyen, H., Liu, B., Auguy, F., Sciallanno, C., Luu, V. T., Dossa, G., S., Cunnac, S., Schmidt, S. M., Slamet-Loedin, I. H., Cruz, C. V., Szurek, B., Frommer, W., B., White, F. F., and Yang, B. 2019. Broad-spectrum resistance to bacterial blight in rice using genome editing. Nat Biotechnol. 37: 1344-1350.

Park, M. R., Seo, J. K., and Kim, K. H. 2013. Viral and nonviral elements in potexvirus replication and movement and in antiviral responses. Adv Virus Res. 87:75-112

Pham, V. N., Kathare, P. K., and Huq, E. 2018. Phytochromes and phytochrome interacting factors. Plant Physiol. 176: 1025-1038.

Prasanth, K. R., Chuang, C., and Nagy, P. D. 2017. Co-opting ATP-generating glycolytic enzyme PGK1 phosphoglycerate kinase facilitates the assembly of viral replicase complexes. PLoS pathog. 13: e1006689.

Rami, N. S., Ismail, P., and Rahmat, A. 2016. Red pitaya juice supplementation ameliorates energy balance homeostasis by modulating obesity-related genes in high- carbohydrate, high-fat diet-induced metabolic syndrome rats. BMC Complement Altern Med. 16:243

Rea, M., Zheng, W., Chen, M., Braud, C., Bhangu, D., Rognan, T. N., and Xiao, W. 2012. Histone H1 affects gene imprinting and DNA methylation in Arabidopsis. Plant J. 71: 776-786.

Rodionova, N. P., Karpova, O. V., Kozlovsky, S. V., Zayakina, O. V., Arkhipenko, M. V., and Atabekov, J. G. 2003. Linear remodeling of helical virus by movement protein binding. J. Mol. Biol. 333:565-572.

doi:10.6342/NTU202003267

Rombolá-Caldentey, B., Rueda-Romero, P., Iglesias-Fernández, R., Carbonero, P., and Oñate-Sánchez, L. 2014. Arabidopsis DELLA and two HD-ZIP transcription factors regulate GA signaling in the epidermis through the L1 box cis-element. Plant Cell. 26: 2905-2919.

Rouleau, M., Smith, R. J., Bancroft, J. B., and Mackie, G. A. 1995. Subcellular immunolocalization of the coat protein of two potexviruses in infected *Chenopodium quinoa*. Virology 214:314-318.

Söderman, E., Mattsson, J., and Engström, P. 1996. The Arabidopsis homeobox gene *ATHB-7* is induced by water deficit and by abscisic acid. Plant J. 10: 375-381.

Sonawane, M. S. 2017. Nutritive and medicinal value of dragon fruit. Asian J. Hort. 12:267–271.

Song, H., Zheng, Z., Wu, J., Lai, J., Chu, Q., and Zheng, X. 2016. White Pitaya (*Hylocereus undatus*) juice attenuates insulin resistance and hepatic steatosis in diet-induced obese mice. Plos. One. 11: e0149670.

Tian, H., Chen, S., Yang, W., Wang, T., Zheng, K., Wang, Y., Cheng, Y., Zhang, N., Liu, S., Li, D., Liu, B., and Wang, S. 2017. A novel family of transcription factors conserved in angiosperms is required for ABA signalling. Plant Cell Environ. 40: 2958-2971.

Voinnet, O., Lederer, C., and Baulcombe, D. C. 2000. A viral movement protein prevents spread of the gene silencing signal in *Nicotiana benthamiana*. Cell 103:157-167

Wang, X., Cao, X., Liu, M., Zhang, R., Zhang, X., Gao, Z., Zhao, X., Xu, K., Li, D., and Zhang, Y. 2018. Hsc70-2 is required for *Beet black scorch virus* infection through interaction with replication and capsid proteins. Sci Rep.

doi:10.6342/NTU202003267

8:1-15.

Wang, X., Goregaoker, S. P., and Culver, J. N. 2009. Interaction of the T*obacco mosaic virus* replicase protein with a NAC domain transcription factor is associated with the suppression of systemic host defenses. J Virol. 83: 9720-9730.

Wieczorek, K., Golecki, B., Gerdes, L., Heinen, P., Szakasits, D., Durachko, D. M., Crosgrove, D. J., Kreil, D. P., Puzio, P. S., Bohlmann, H., and Grundler, F. M. W. 2006. Expansins are involved in the formation of nematode-induced syncytia in roots of *Arabidopsis thaliana*. Plant J. 48: 98-112.

Wu, Y.-M. 2019. Investigation of the synergistic interaction between *Cactus virus X* and *Pitaya virus X*. National Taiwan University. Master thesis.

Xu, M., Liu, C. L., Luo, J., Qi, Z., Yan, Z., Fu, Y., Wei, S.-S., and Tang, H. 2019. Transcriptomic *de novo* analysis of pitaya (*Hylocereus polyrhizus*) canker disease caused by *Neoscytalidium dimidiatum*. BMC genomics. 20:10.

Yoshida, T., Nishimura, N., Kitahata, N., Kuromori, T., Ito, T., Asami, T., Shinozaki, K., and Hirayama, T. 2006. *ABA-hypersensitive germination3* encodes a protein phosphatase 2C (AtPP2CA) that strongly regulates abscisic acid signaling during germination among Arabidopsis protein phosphatase 2Cs. Plant physiol. 140: 115-126.

Zhuang, Y., Zhang, Y., and Sun, L. 2012. Characteristics of fibre-rich powder and antioxidant activity of pitaya (*Hylocereus undatus*) peels. Int. J. Food Sci. Technol. 47:1279–1285.

doi:10.6342/NTU202003267

Figures

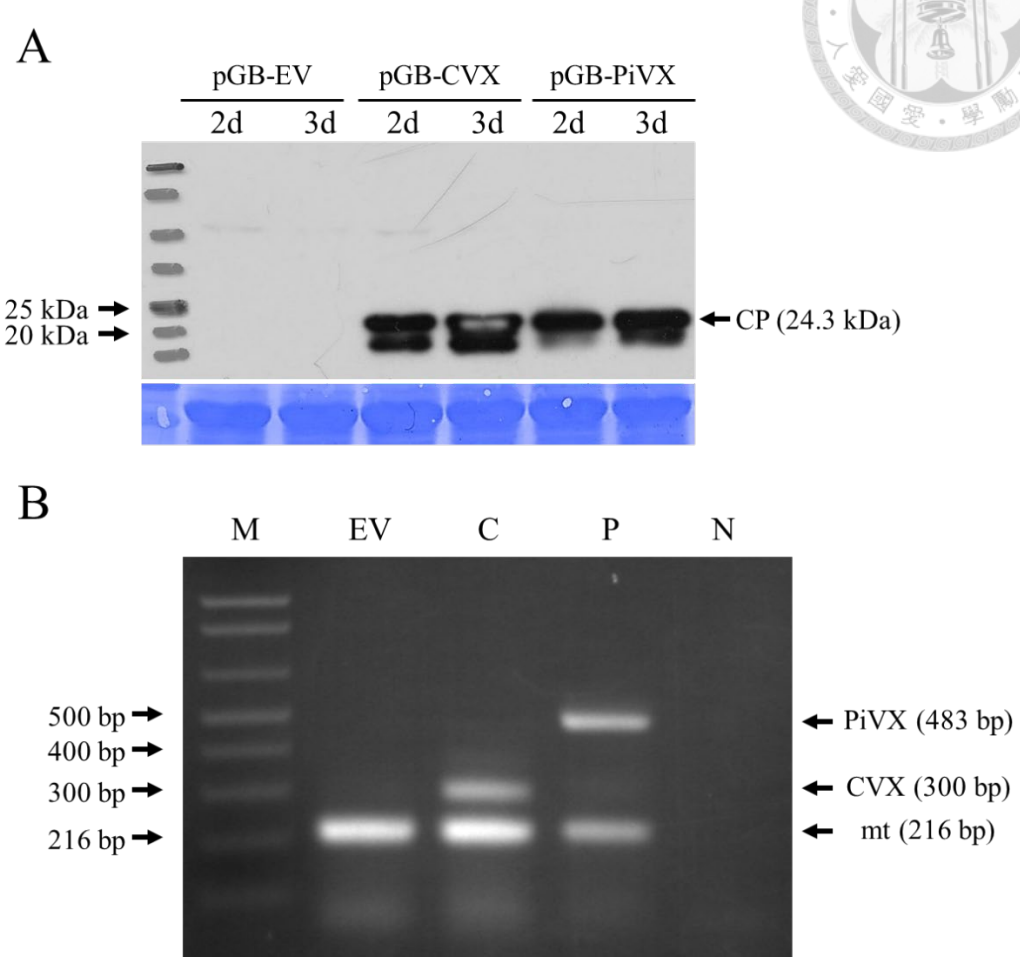

doi:10.6342/NTU202003267

Fig. 1 Detection of CVX and PiVX on agroinfiltrated *Nicotiana benthamiana* plants. A, Western blot analysis of *N. benthamiana* plants at 2 and 3 days post-infiltration. Ten microliters of protein crude extract mixed with 2X sample buffer were loaded into 10% SDS-polyacrylamide gel for electrophoresis. Immunoblot was performed with anti-PiVX CP antibody to detect the coat proteins of CVX and PiVX. Arrow indicates the position of viral coat protein (CP). B, Multiplex RT-PCR of *N. benthamiana* plants at 2 days post-infiltration. EV: empty vector. C: CVX-infiltrated plants. P: PiVX-infiltrated plants. N: negative control. Arrows indicate the positions of RT-PCR products of mitochondria (mt), CVX and PiVX.

doi:10.6342/NTU202003267

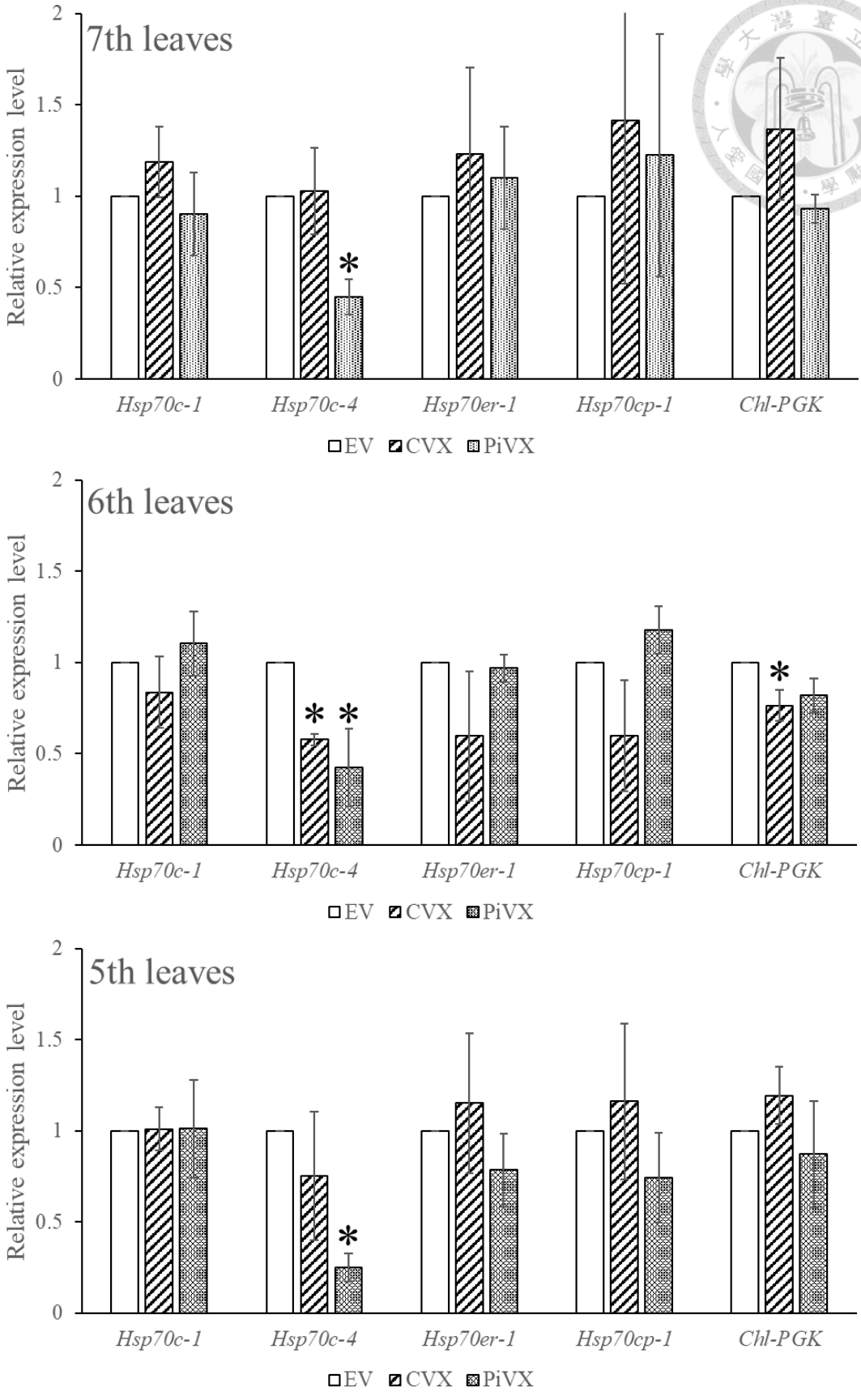

doi:10.6342/NTU202003267

Fig. 2 Relative expression levels of potential host factors at different agroinfiltrated *N. benthamiana* leaves. Empty vector-, CVX- and PiVX-infiltrated leaves were harvested at 2 days post-infiltration and total RNAs were purified. Results of semiquantitative RT-PCR were quantified by Image J. Asterisks indicate significant differences (p value ≤ 0.05) between mock and CVX- or PiVX-infiltrated leaves calculated by Student's t-test. The data represent at least two independent experiments.

doi:10.6342/NTU202003267

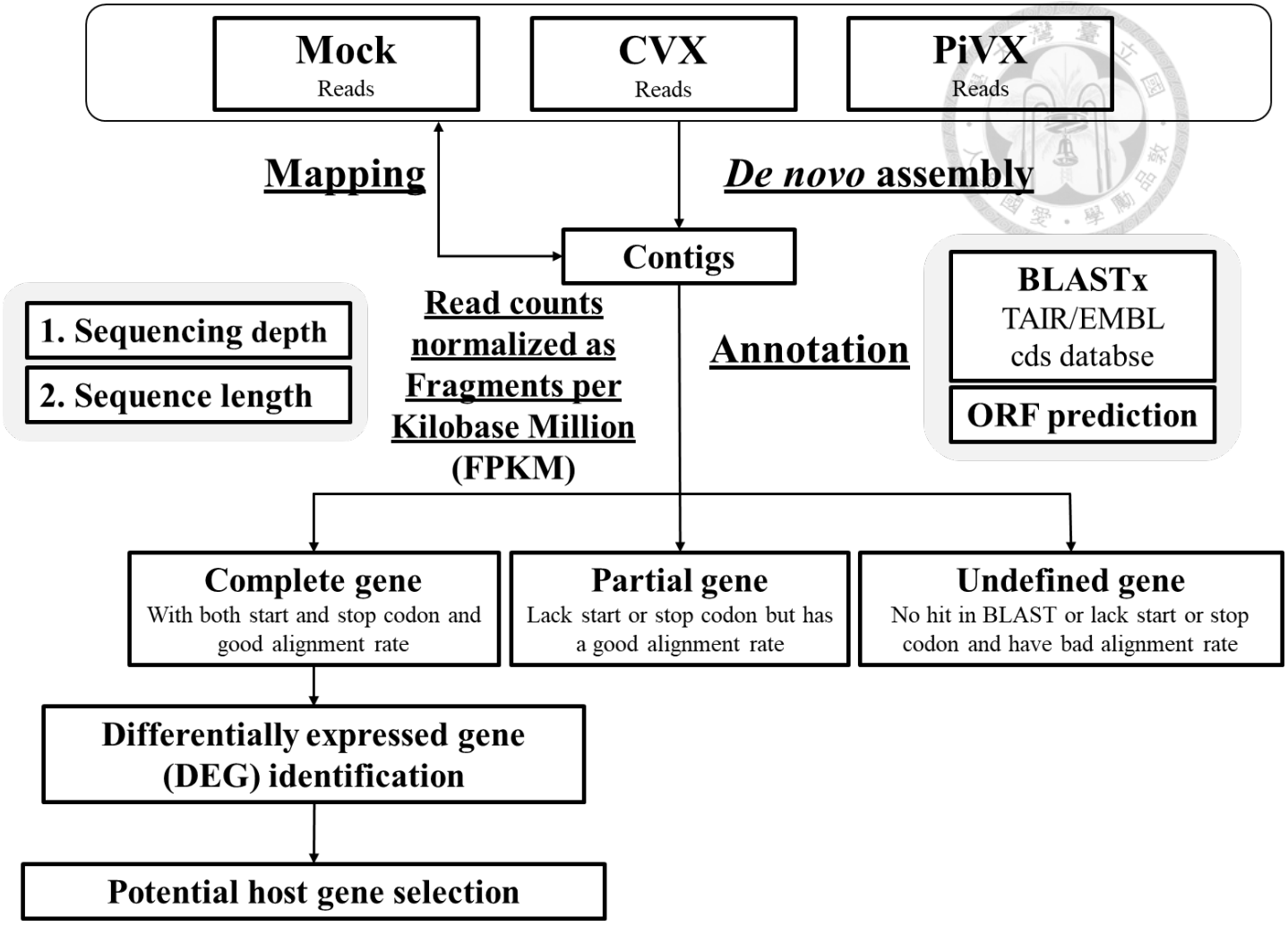

Fig. 3 Workflow of preliminary transcriptome analysis. All reads from mock, CVX-and PiVX-infected treatments were assembled into contigs using *de novo* assembly method. The contigs were than annotated using BLASTx and ORF prediction tools, and the FPKM values were calculated. The identified complete genes were than used for differentially expressed gene (DEG) identification followed by potential host gene selection.

doi:10.6342/NTU202003267

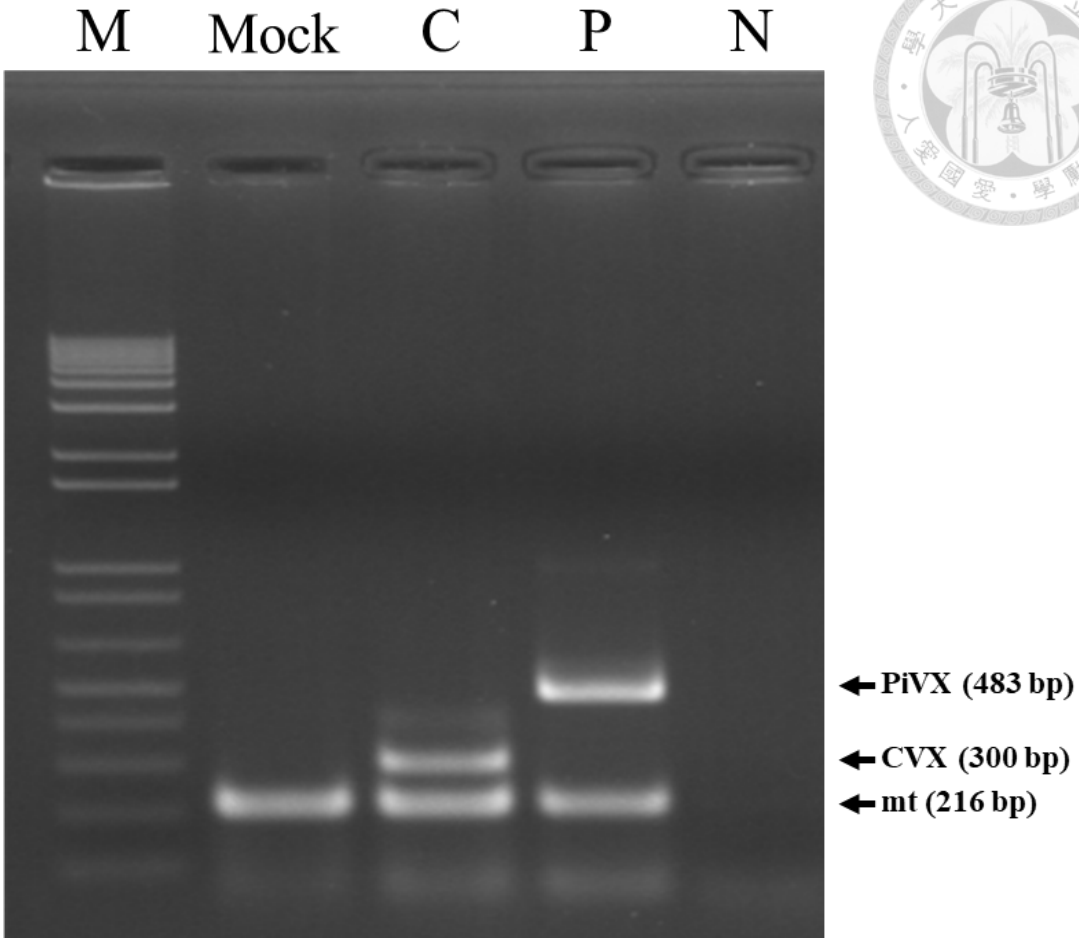

Fig. 4 Detection of CVX and PiVX on inoculated pitaya plants. Multiplex RT-PCR of pitaya cotyledons at 17 days post-inoculation. C: CVX-infected plants. P: PiVX-infected plants. N: negative control. Arrows indicate the positions of amplified products of mitochondria (mt), CVX and PiVX.

doi:10.6342/NTU202003267

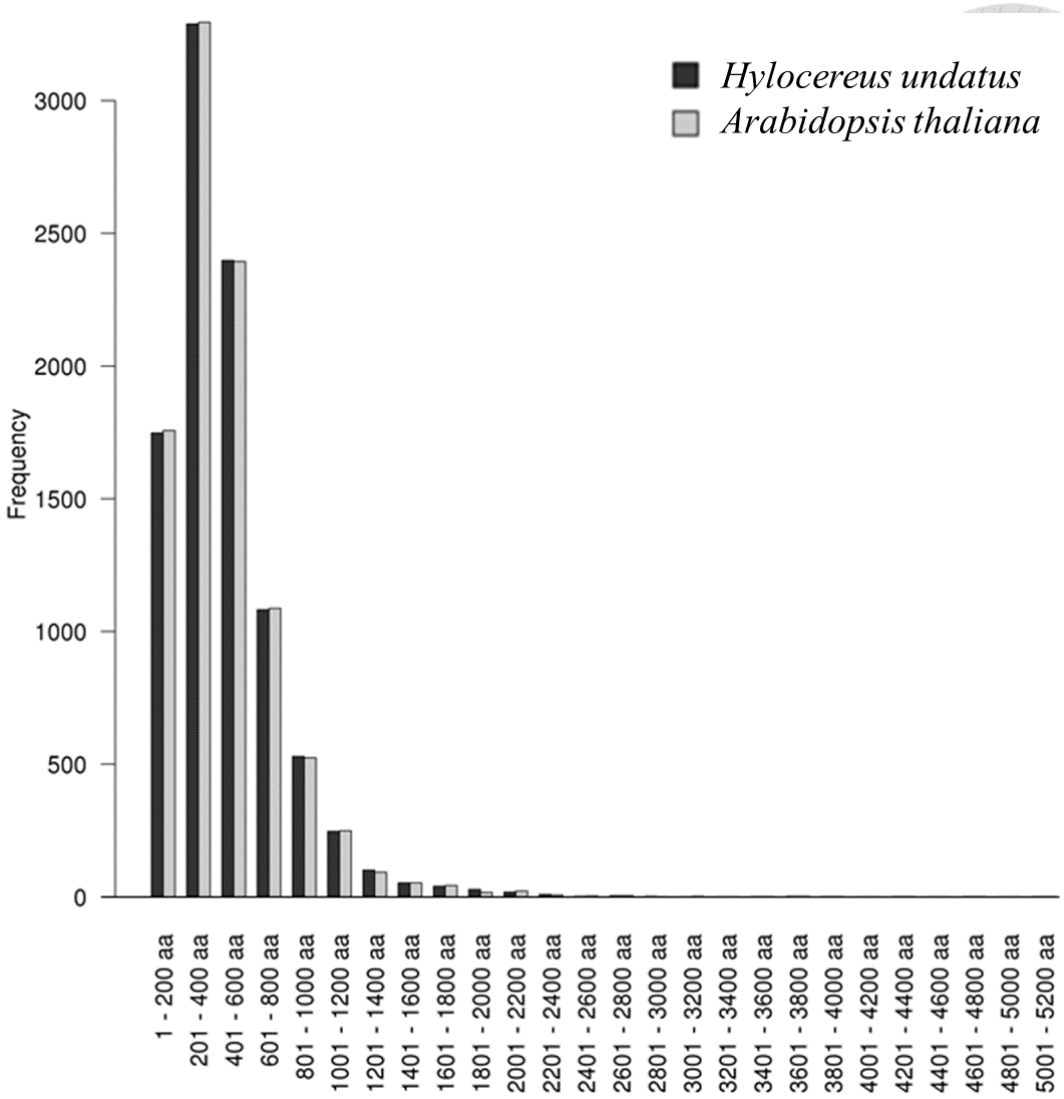

Fig. 5 The length distribution comparison of the protein sequences of pitaya (*Hylocereus undatus*) and Arabidopsis in preliminary transcriptome. The horizontal axis represents amino acid lengths, and the vertical axis represents the occurring frequency. Black column represents pitaya genes while gray column represents the reference Arabidopsis genes.

doi:10.6342/NTU202003267

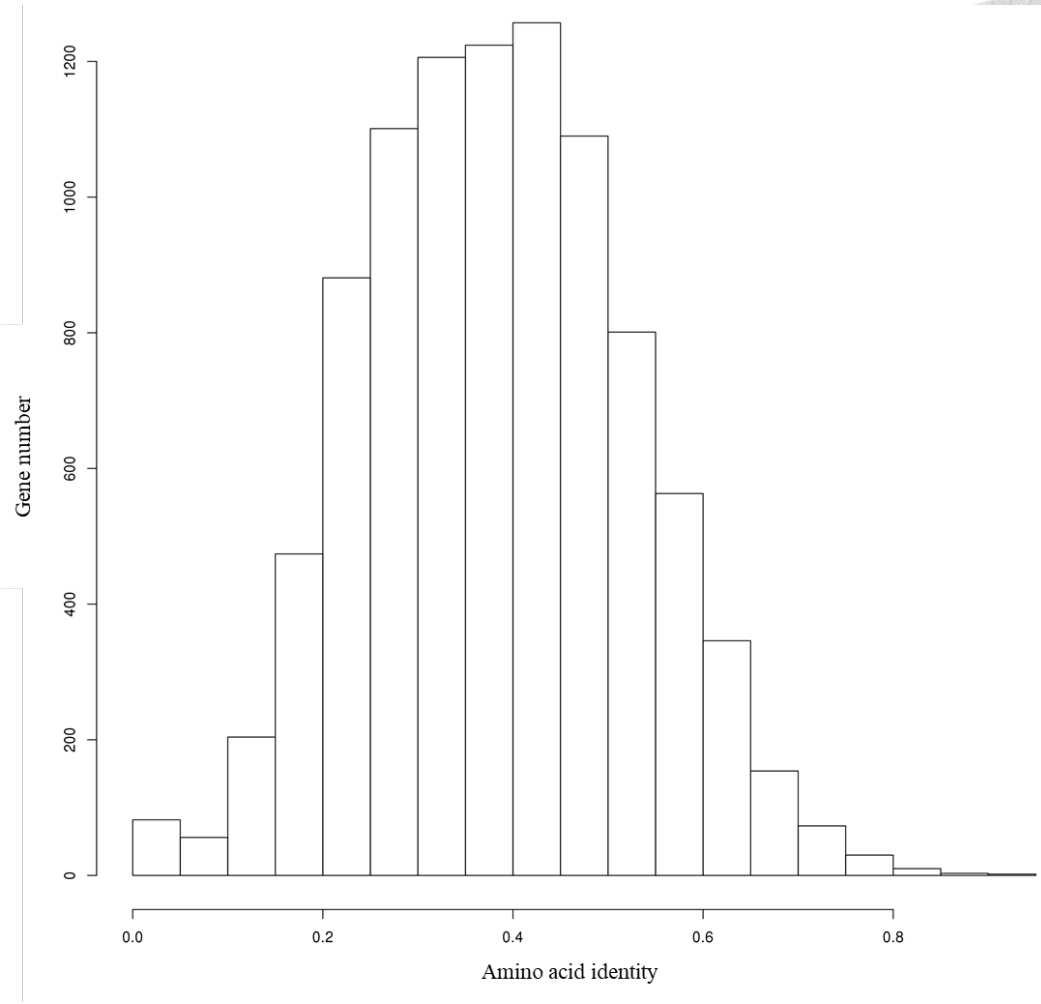

Fig. 6 Amino acid identity of the amino acid sequences of pitaya (*Hylocereus undatus*) and Arabidopsis in preliminary transcriptome. Horizontal axis indicates the sequence identity between pitaya and Arabidopsis, and the vertical axis represents the occurring frequency.

doi:10.6342/NTU202003267

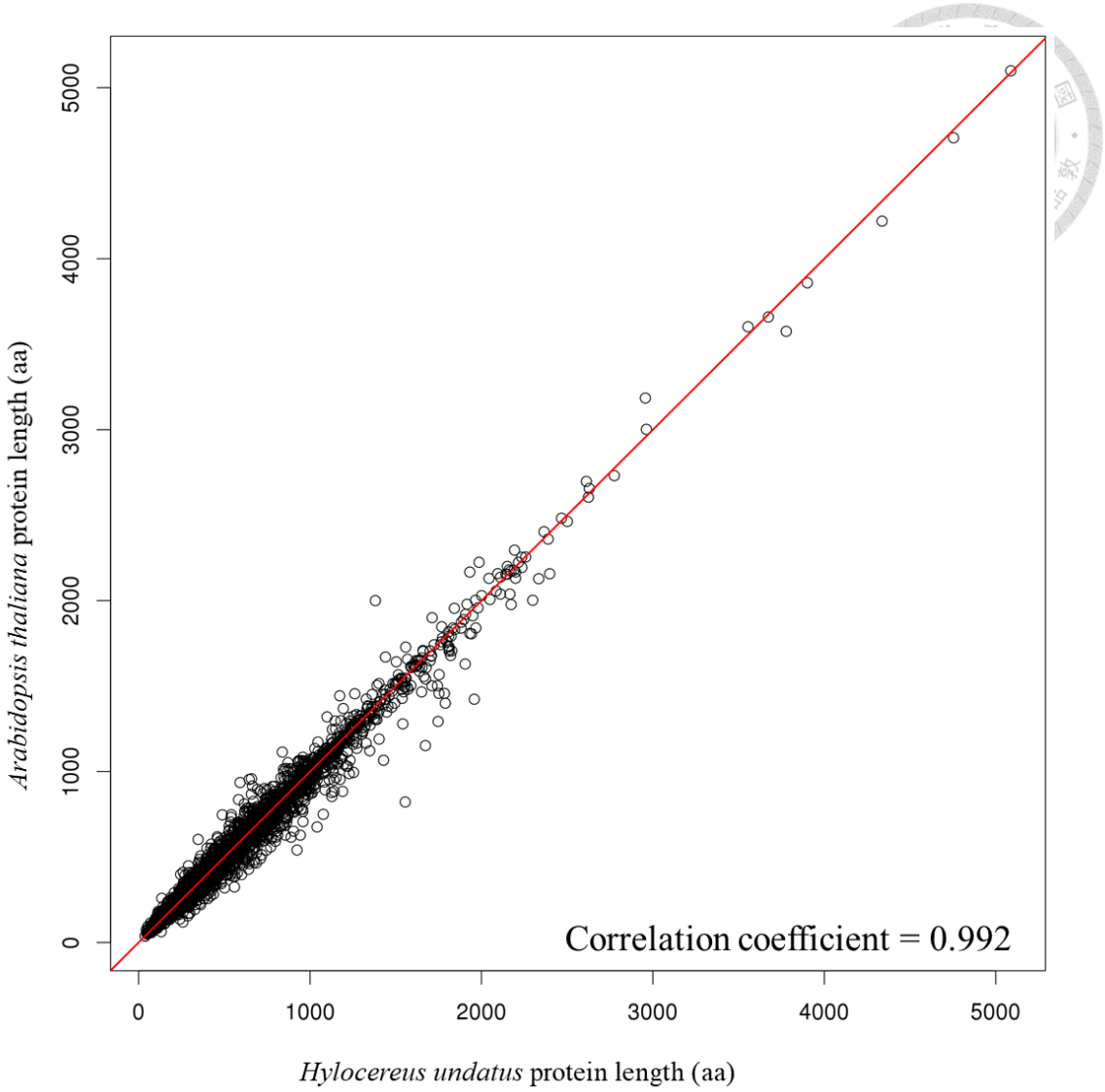

Fig. 7 Scatter plot of the protein sequence length of pitaya (*Hylocereus undatus*) and Arabidopsis in preliminary transcriptome. The horizontal axis represents the lengths of pitaya protein sequences, and the vertical axis indicates the lengths of Arabidopsis protein sequences. Correlation coefficient is 0.992.

doi:10.6342/NTU202003267

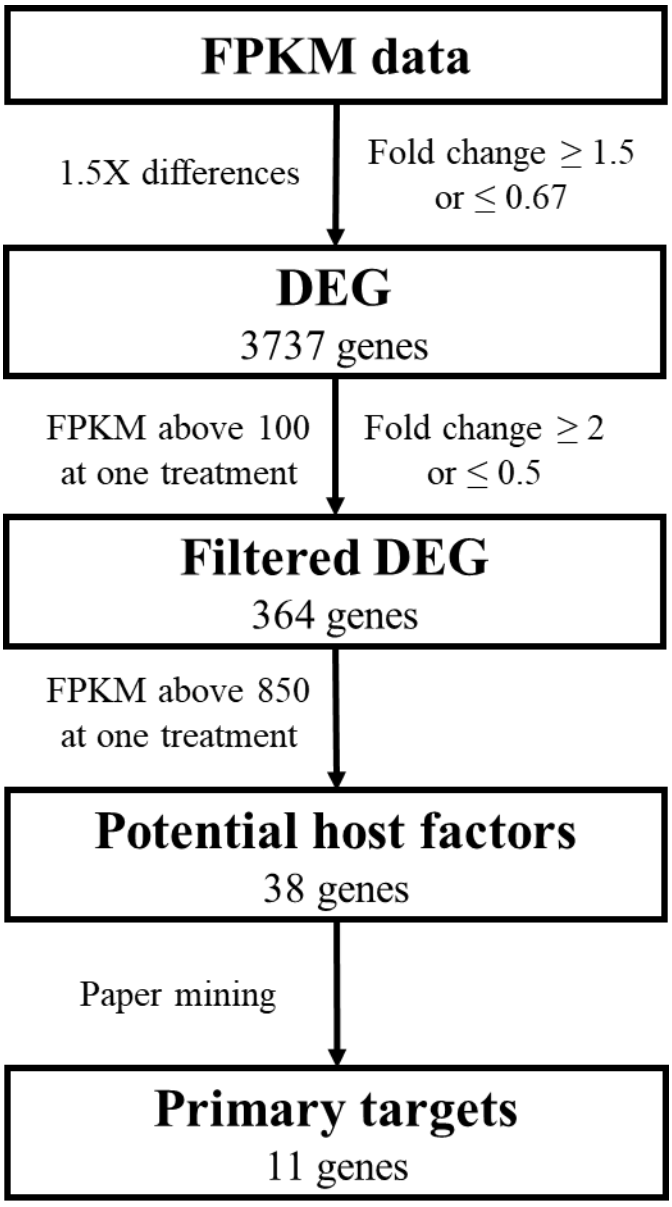

Fig. 8 Flowchart of pitaya primary target identification procedures. DEGs were identified as complete genes with fold change ≥ 1.5 or ≤ 0.67 between mock and virus-infected treatment. The DEGs were then further filtered by changing FPKM parameters to determine potential host factors. Finally, the remaining genes were reviewed and then selected as pitaya primary targets during virus infection.

doi:10.6342/NTU202003267

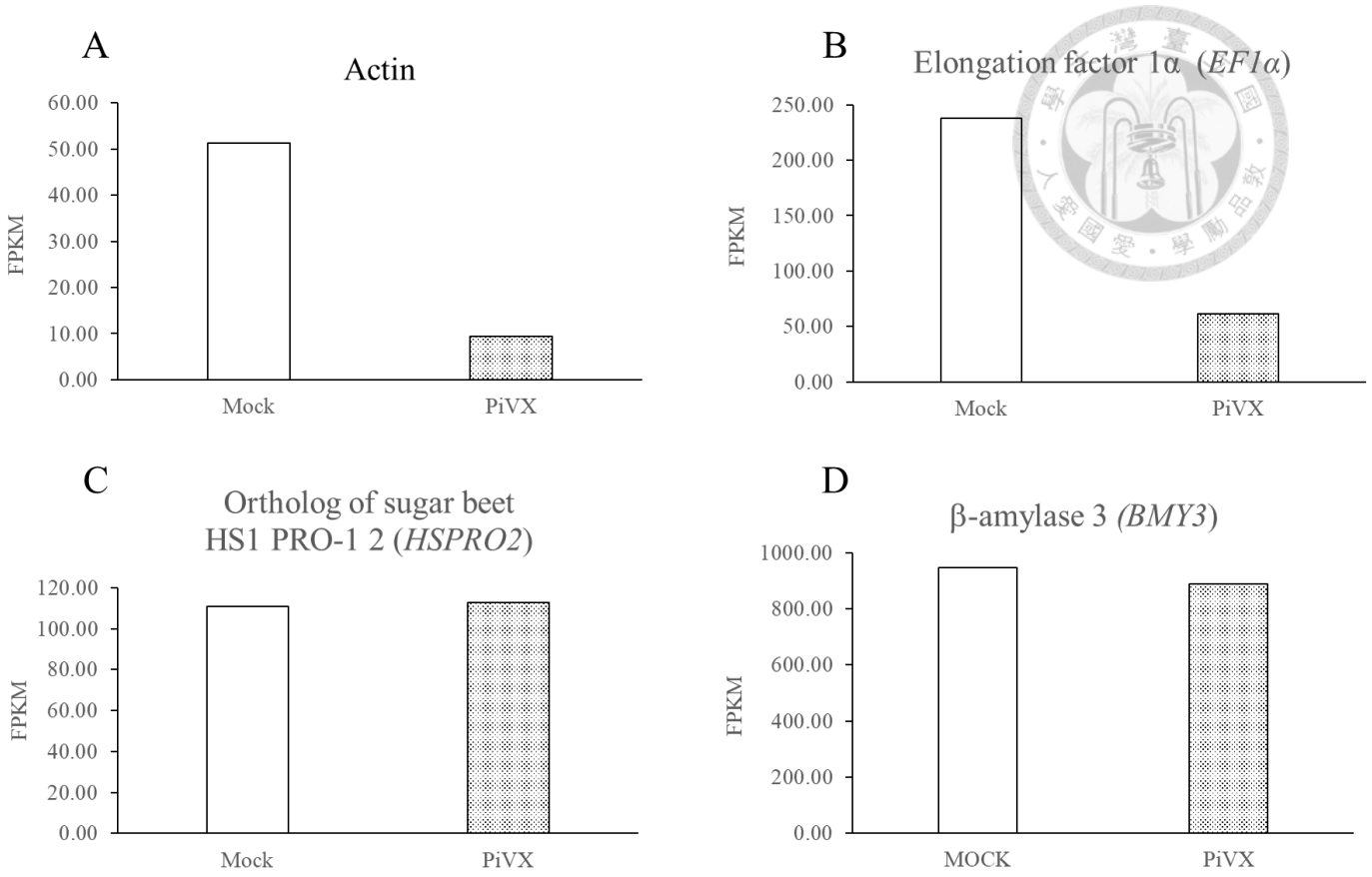

Fig. 9 Expression levels of potential reference genes for quantitative RT-PCR in mock and PiVX-infected pitayas. The FPKM values of commonly used reference genes, *actin* (A) and *elongation factor 1 alpha* (*EF-1α*) (B), and potential pitaya reference genes, *ortholog of sugar beet HS1 PRO-1 2* (*HSPRO2*) (C) and *Beta amylase 3* (*BMY3*) (D) of mock and PiVX treatments were shown.

doi:10.6342/NTU202003267

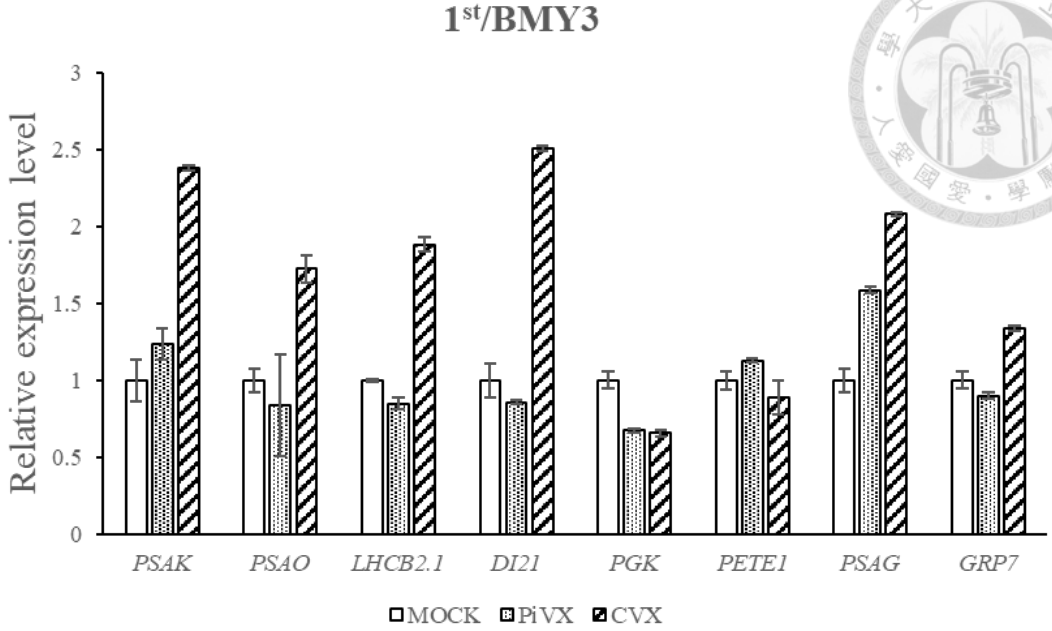

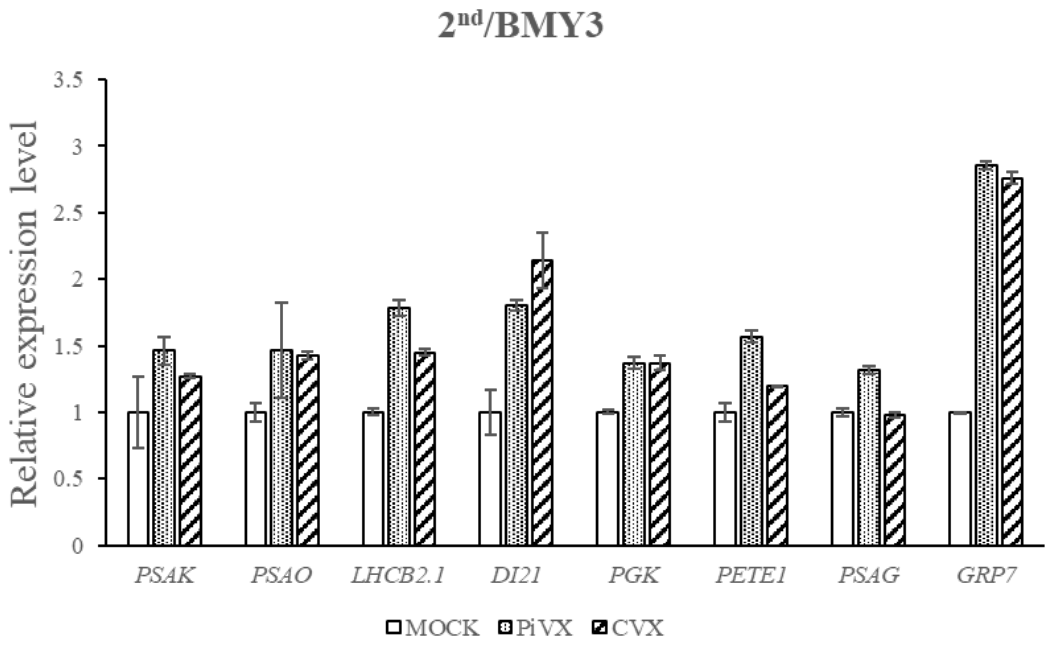

doi:10.6342/NTU202003267

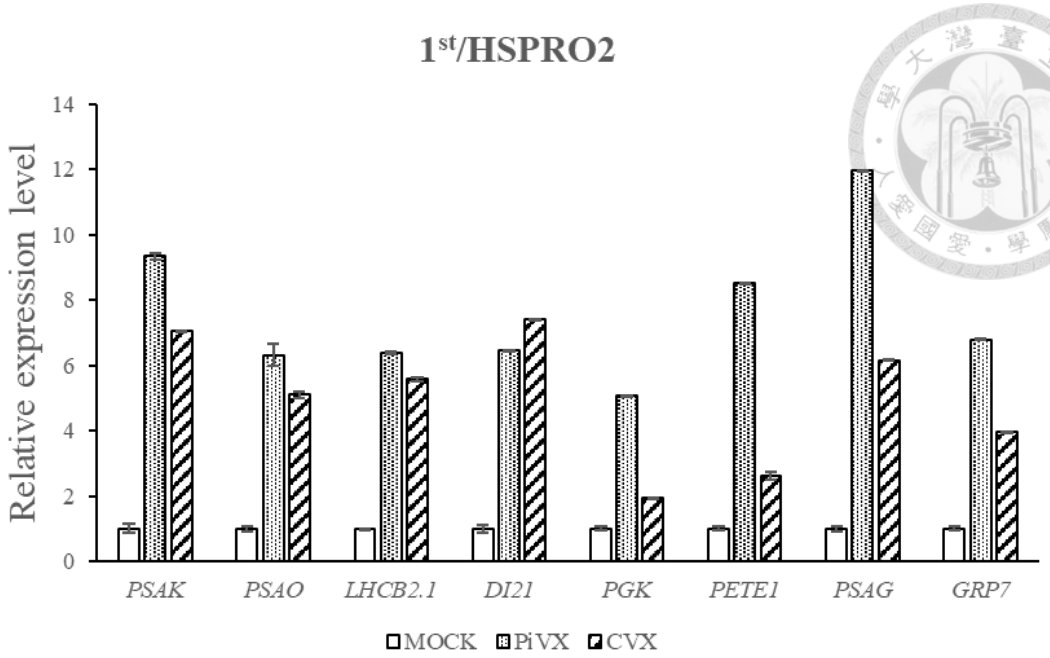

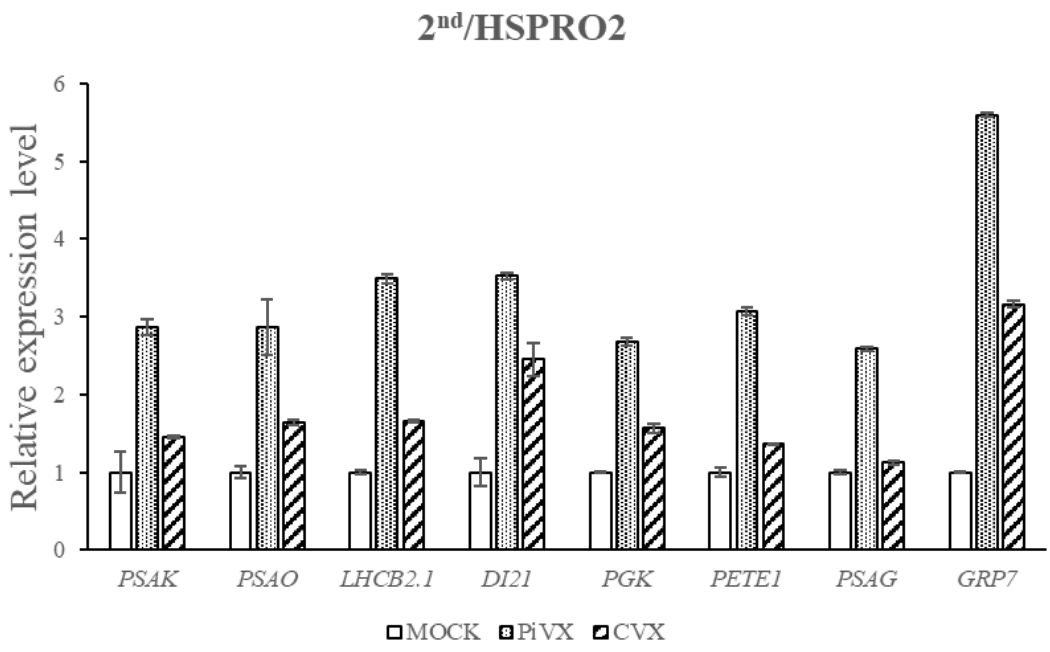

doi:10.6342/NTU202003267

Fig. 10 Validation of the expression levels of few potential host factors of pitaya. Mock, CVX- and PiVX-inoculated pitaya samples were harvested at 17 dpi, and total RNAs were analyzed by RT-qPCR. Two independent experiments were performed. Relative expression levels of few primary targets were measured by RT-qPCR using two potential reference genes *BMY3* and *HSPRO2*, respectively. The figures were generated based on 3 repeats for each treatments and genes, and standard deviation values were calculated.

doi:10.6342/NTU202003267

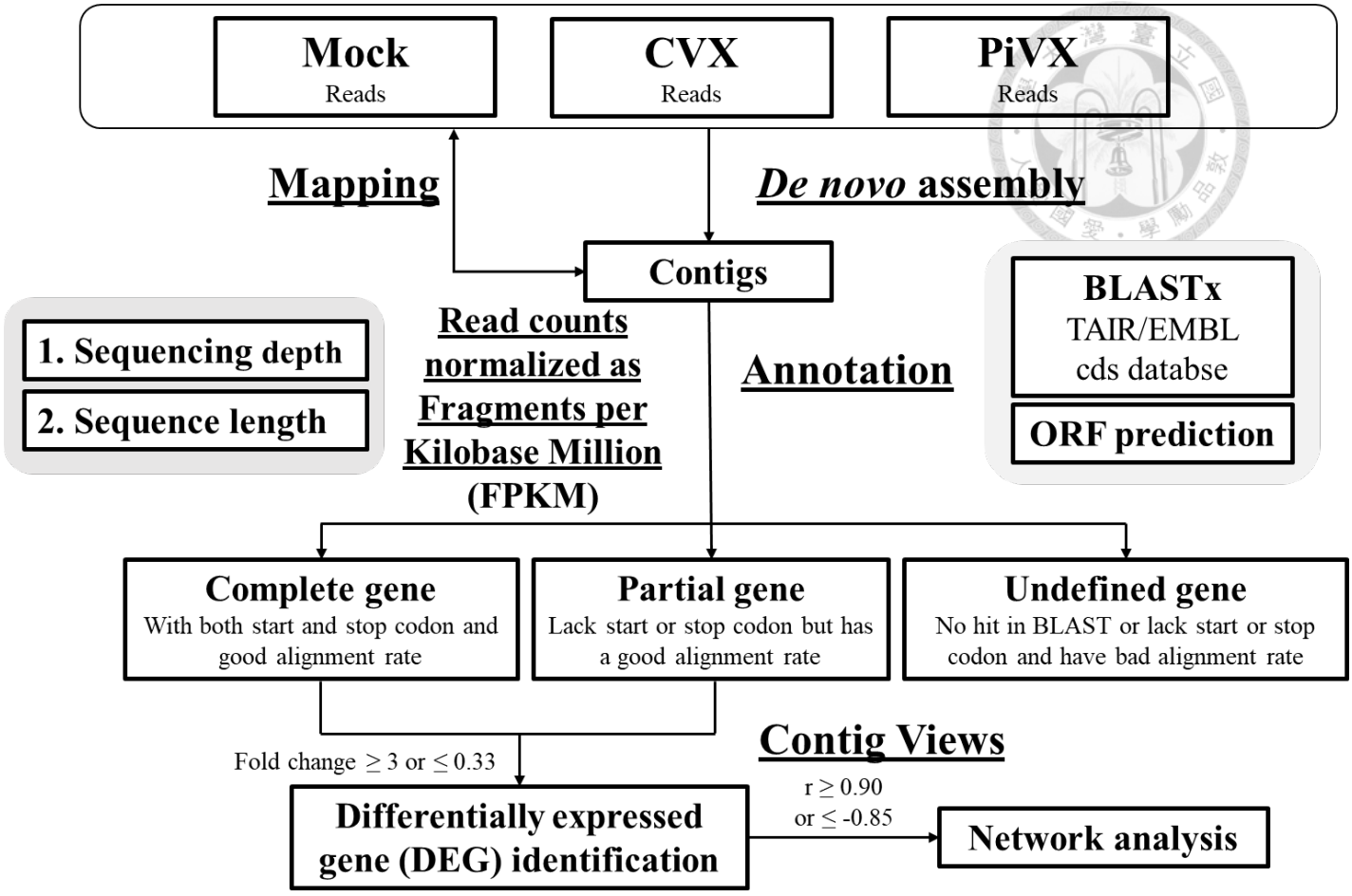

Fig. 11 Workflow of full transcriptome analysis. All reads from the three times sequencing results of mock, CVX-and PiVX-infected RNAs were assembled into contigs using *de novo* assembly method. The contigs were than annotated using BLASTx and ORF prediction tools, and the FPKM values were calculated. Complete genes and partial genes were used for DEG identification and network analysis.

doi:10.6342/NTU202003267

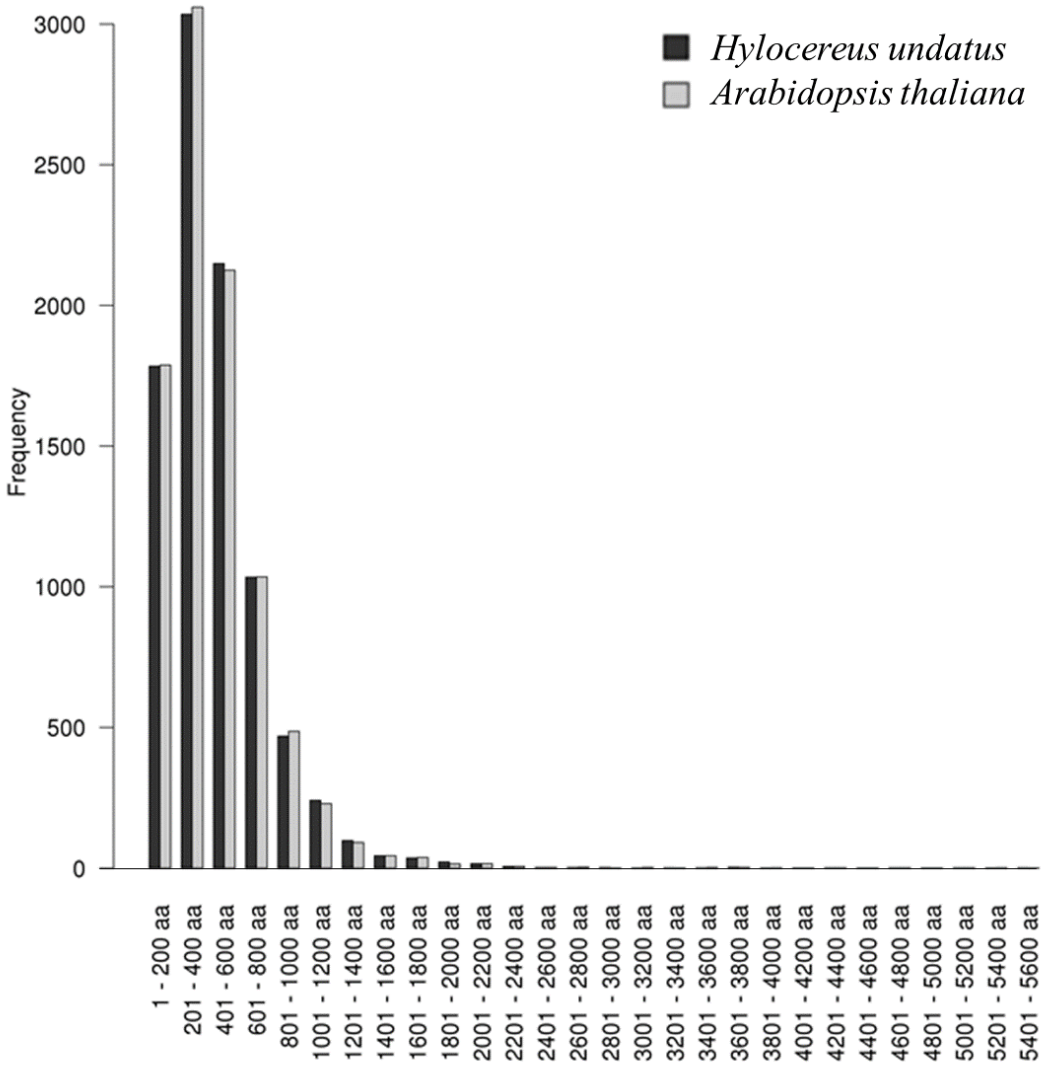

Fig. 12 The length distribution comparison of the coding sequences of pitaya (*Hylocereus undatus*) and Arabidopsis in full transcriptome. The horizontal axis represents amino acid lengths, and the vertical axis represents the occurring frequency. Black column represents pitaya genes while gray column represents the reference Arabidopsis genes.

doi:10.6342/NTU202003267

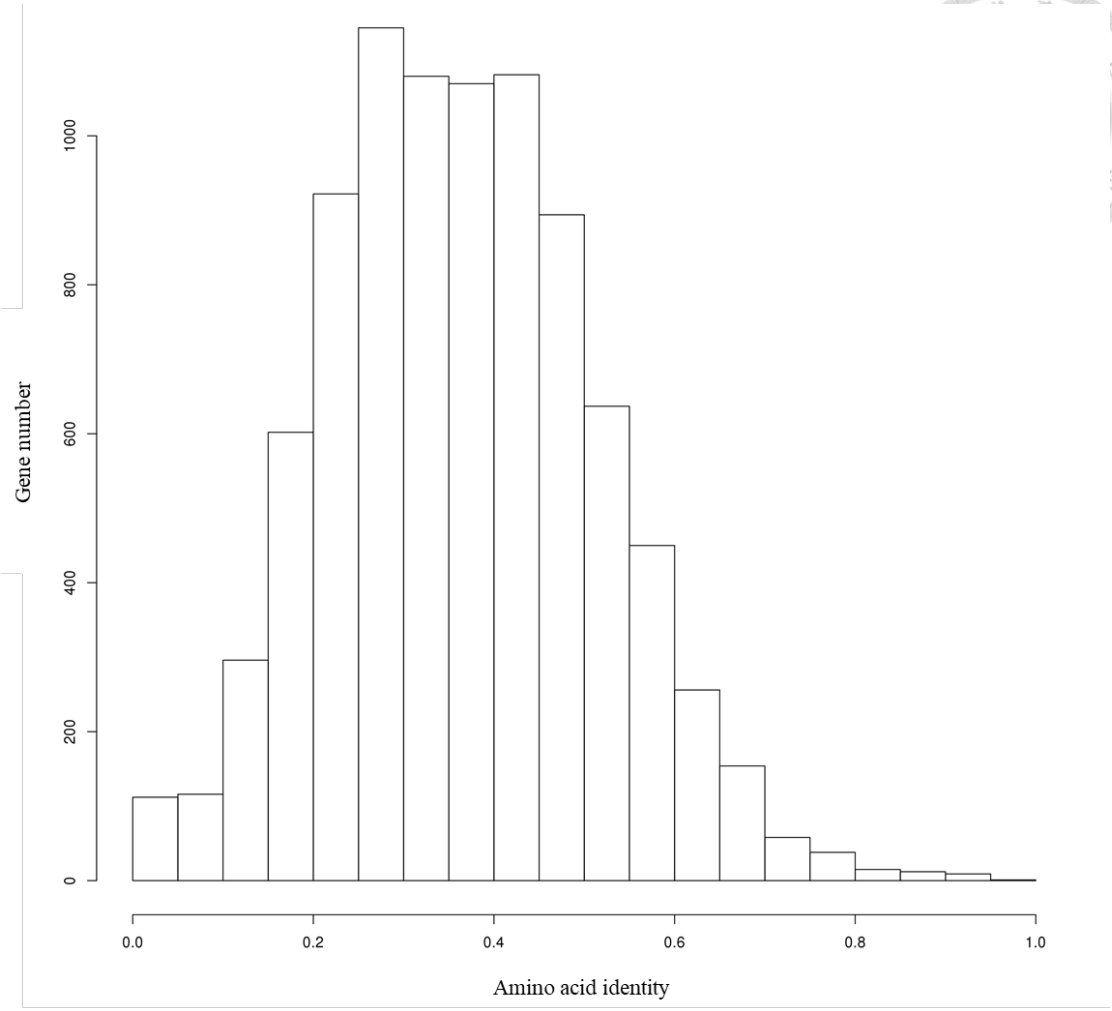

Fig. 13 Amino acid identity of the coding sequences of pitaya (*Hylocereus undatus*) and Arabidopsis in full transcriptome. Horizontal axis indicates the sequence identity between pitaya and Arabidopsis, and the vertical axis represents the occurring frequency.

doi:10.6342/NTU202003267

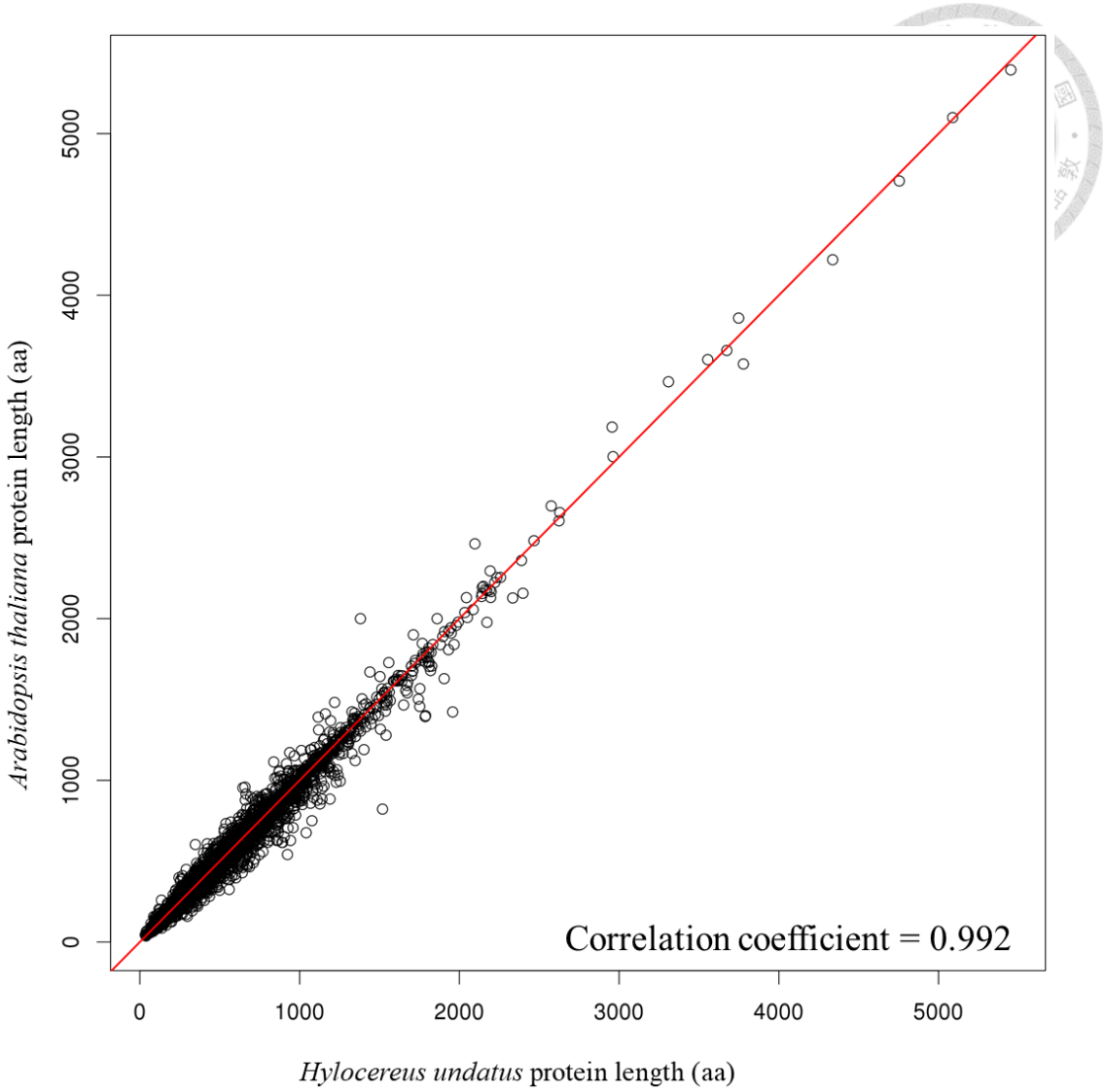

Fig. 14 Scatter plot of the protein sequence length of pitaya (*Hylocereus undatus*) and Arabidopsis in full transcriptome. The horizontal axis represents lengths of pitaya protein sequences, and the vertical axis indicates lengths of Arabidopsis protein sequences.

doi:10.6342/NTU202003267

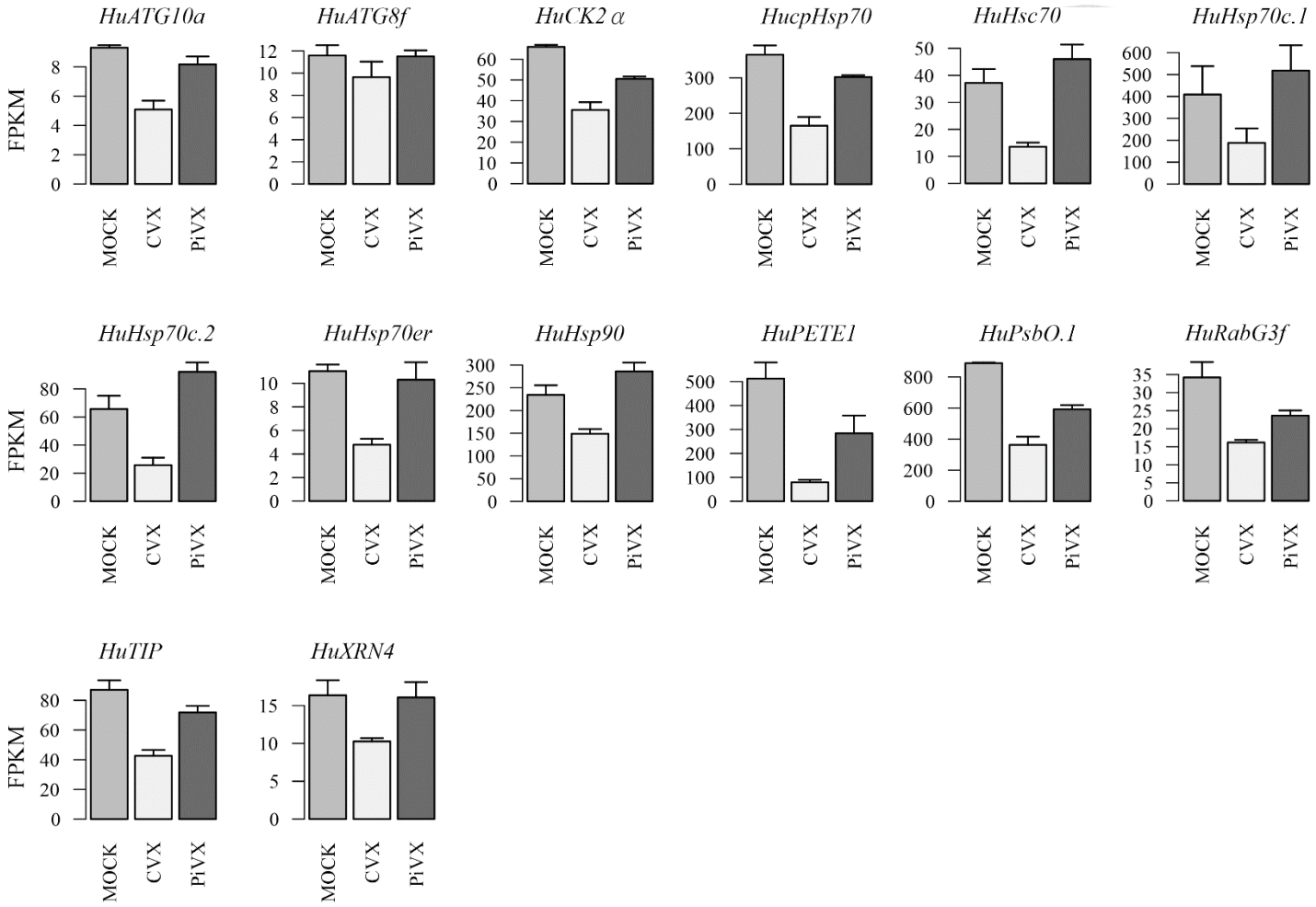

Fig. 15 Expression levels of potential potexvirus host factors in full transcriptome. Expression levels of the best-matched pitaya genes with the reported potexvirus host factors were shown as FPKM with SE value calculated. *HuATG10a*, PTYV3_7809. *HuATG8f*, PTYV3_7768. *HuCK2α*, PTYV3_4131. *HucpHsp70*, PTYV3_709. *HuHsc70*, PTY1533. *HuHsp70c.1*, PTYV3_1019. *HuHsp70c.2*, PTYV3_1546. *HuHsp70er*, PTYV3_928. *HuHsp90*, PTYV3_1850. *HuPETE1*, PTYV3_336. *HuPsbO.1*, PTYV3_503. *HuRabG3f*, PTYV3_25391. *HuTIP*, PTYV3_3482. *HuXRN4*, PTYV3_18032.

doi:10.6342/NTU202003267

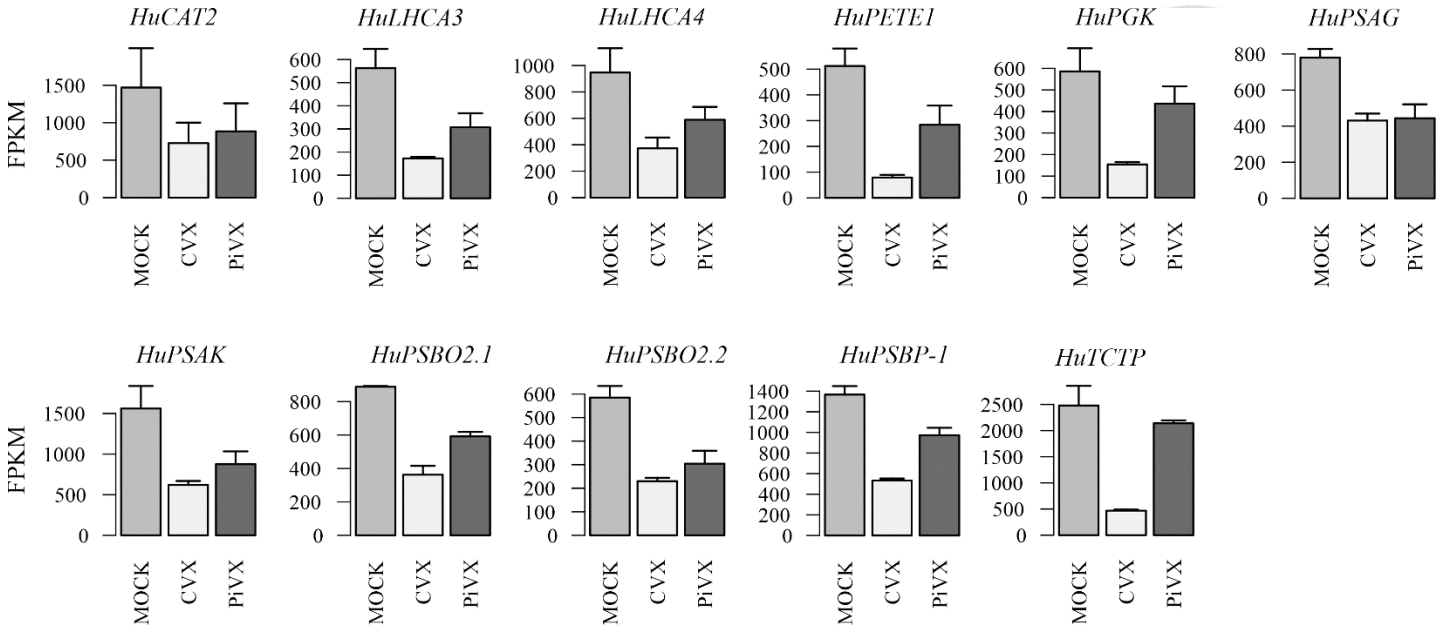

Fig. 16 Expression levels of previously selected pitaya primary targets in full transcriptome. Expression levels of ten previously selected primary targets were shown as FPKM with SE value calculated. *HuCAT2*, PTY243. *HuLHCA3*, PTY898. *HuLHCA4*, PTY141. *HuPETE1*, PTY398. *HuPGK*, PTY189. *HuPSAG*, PTY1299. *HuPSAK*, PTY961. *HuPSBO2.1*, PTY642. *HuOSBO2.2*, PTY825. *HuPSBP-1*, PTY471. *HuTCTP*, PTY607.

doi:10.6342/NTU202003267

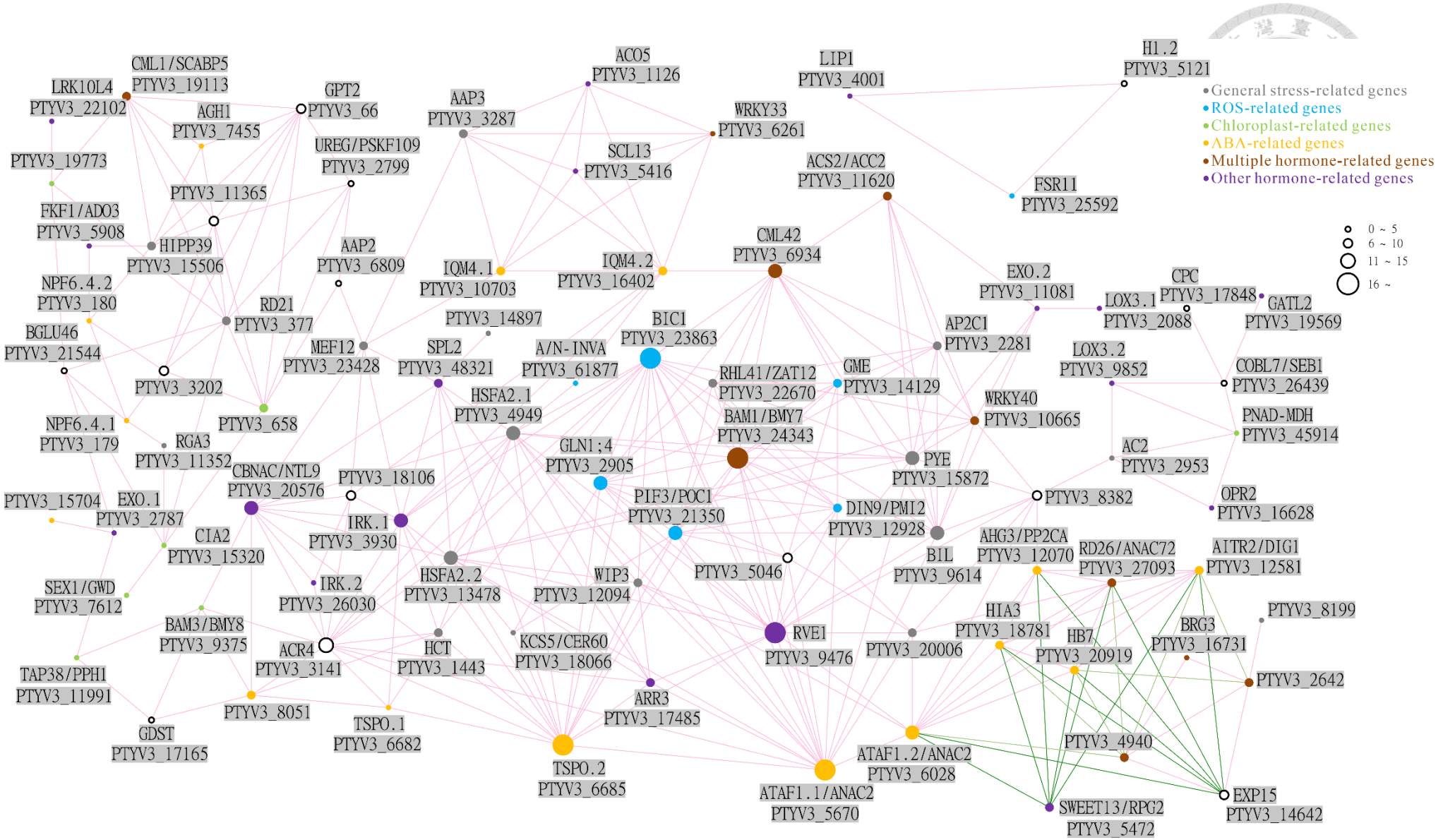

doi:10.6342/NTU202003267

Fig. 17 Full PiVX infection network. Differential expressed genes that showed at least 3 times differences between Mock and PiVX treatment were picked and Pearson correlation coefficient of these genes were calculated using all 9 samples including those of CVX. Each circle represents a gene and the line indicates relation between the genes. Red line, positive relation ($r \geq 0.9$). Green line, negative relation ($r \leq -0.85$). Genes were colored based on their classification and the size of a gene is proportional to how many connections the gene has.

doi:10.6342/NTU202003267

A

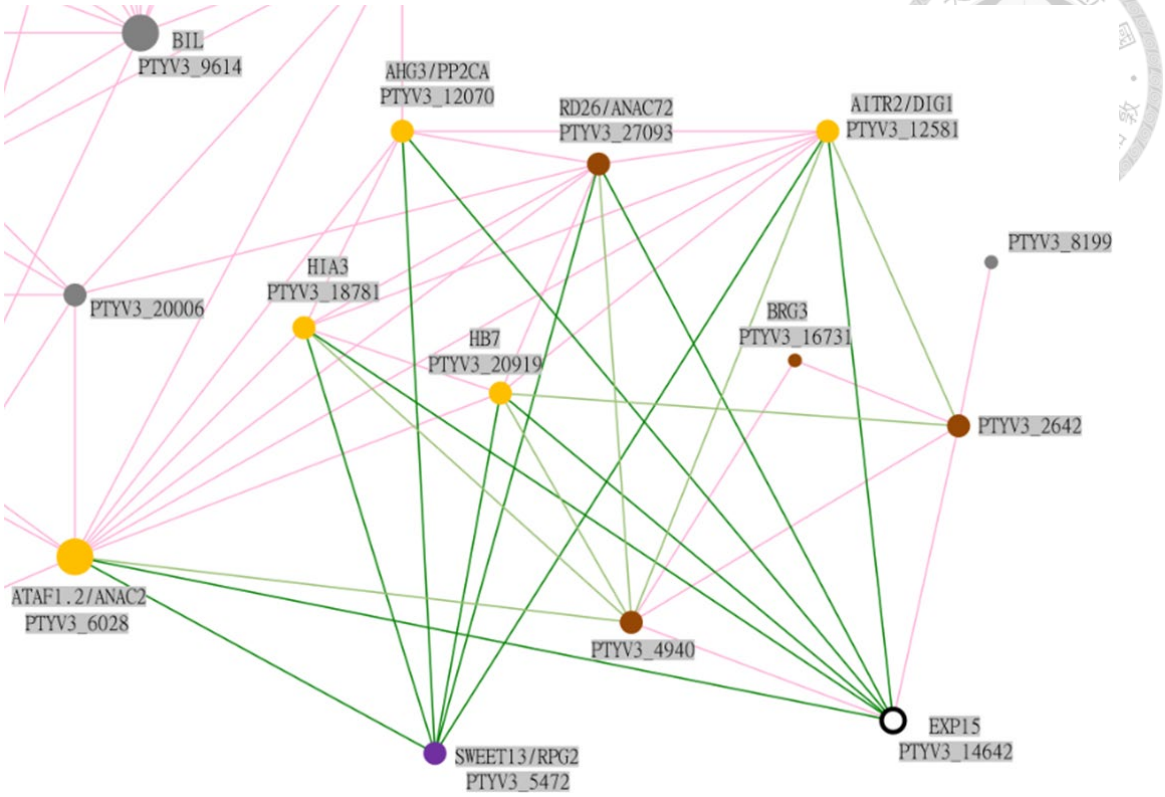

B

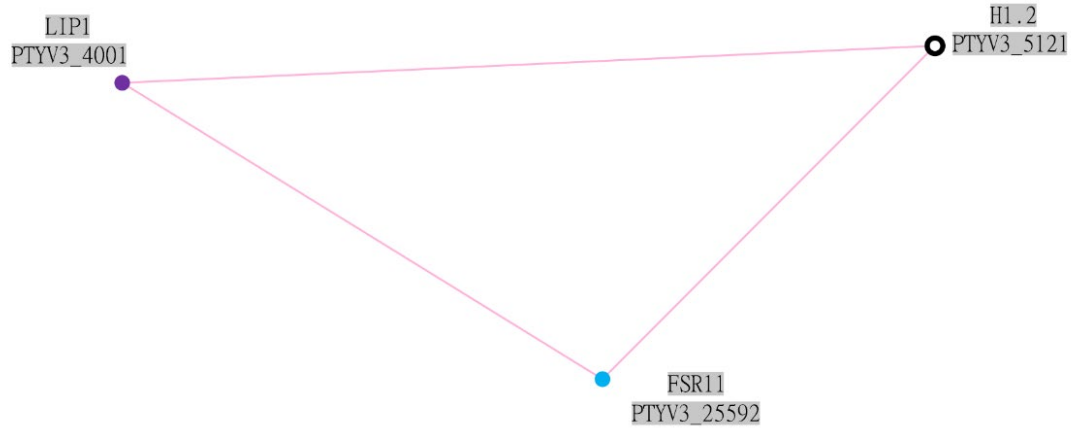

doi:10.6342/NTU202003267

Fig. 18 Detailed PiVX infection network. Each circle represents a gene and the line indicates relation between the genes. Red line, positive relation. Green line, negative relation. Genes were colored based on their classification and the size of a gene is proportional to how many connections the gene has. A, Network region with negative relation between the genes (bottom right of Fig. 17). B, Network region with three distinct genes (top right of Fig. 17).

doi:10.6342/NTU202003267

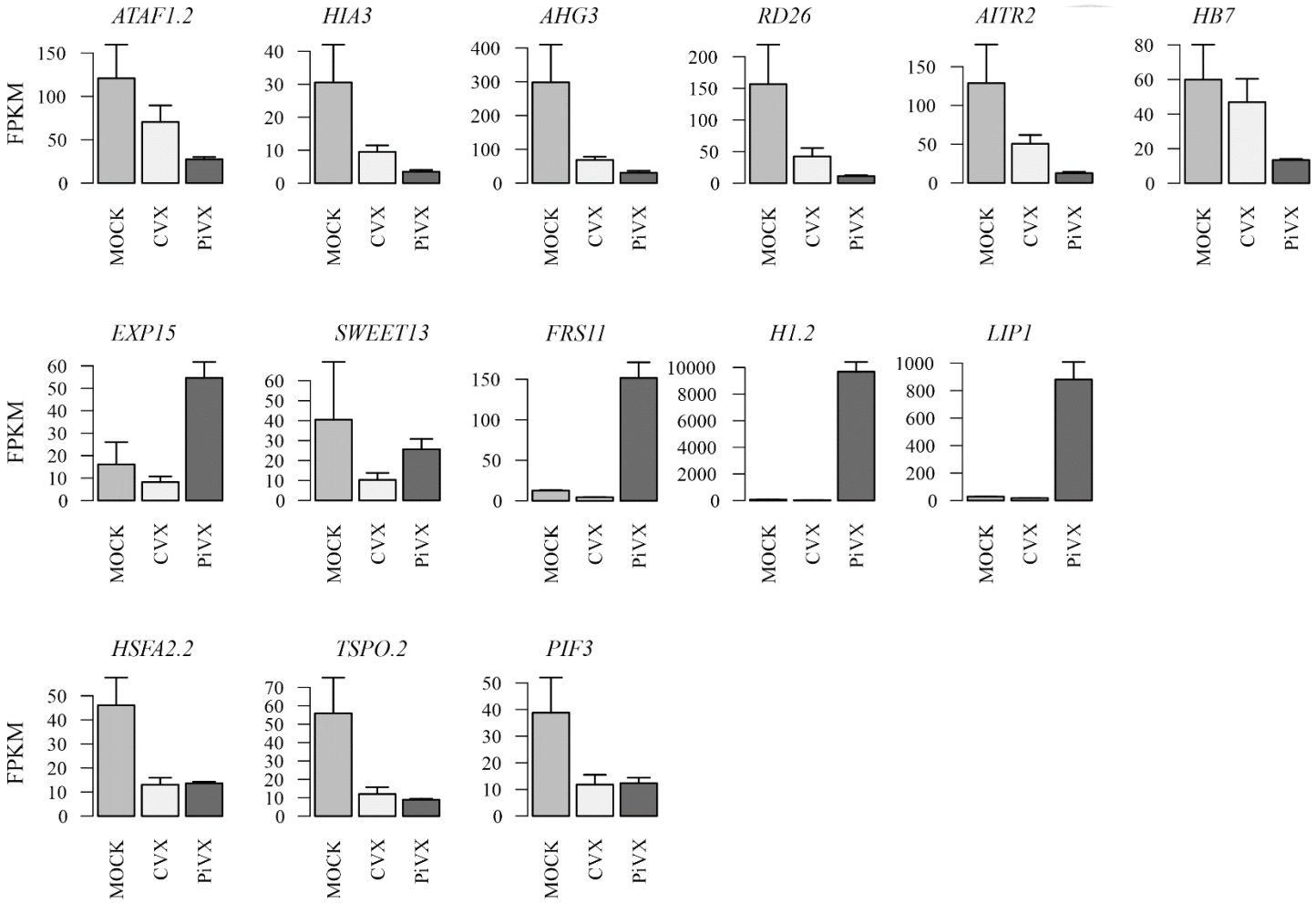

.

Fig. 19 Expression levels of genes discussed in the PiVX and CVX infection network. Expression levels of the genes are shown as FPKM with SE value calculated. A, Genes discussed in the PiVX infection network. B, Common genes discussed in CVX and PiVX infection networks. *ATAF1.2*, PTYV3_6028. *HIA3*, PTYV3_18781. *AHG3*, PTYV3_12070. *RD26*, PTYV3_27093. *AITR2*, PTYV3_12581. *HB7*, PTYV3_20919. *EXP15*, PTYV3_14642. *SWEET13*, PTYV3_5472. *FRS11*, PTYV3_25592. *H1.2*, PTYV3_5121. *LIP1*, PTYV3_4001. *HSFA2.2*, PTYV3_13478. *TSPO.2*, PTYV3_6685. *PIF3*, PTYV3_21350.

doi:10.6342/NTU202003267

Tables

Table 1 Previously reported host genes related to potexviruses

Host factor	Regulation by virus	Virus	Reference
ATG10a[a]	Upregulation	BaMV	Huang et al. 2019b
ATG5[a]	ND	BaMV	Huang et al. 2019a
ATG8f[a]	Upregulation	BaMV	Huang et al. 2019a
Chl-PGK[a]	ND	BaMV	Cheng et al. 2013a
CK2α[a]	ND	BaMV	Hung et al. 2014
cpHsp70[a]	Upregulation	BaMV	Huang et al. 2017
eEF1a[a]	ND	BaMV	Lin et al. 2007
GSTU4[a]	ND	BaMV	Chen et al. 2013
Hsc70[a, b]	ND	PepMV	Mathioudakis et al. 2014
Hsp70c-1 [a]	Upregulation	PVX	Chen et al. 2008
Hso70c-2 [a]	Upregulation	PVX	Chen et al. 2008
Hsp70c-3 [a]	Upregulation	PVX	Chen et al. 2008
Hsp70c-4 [a]	Upregulation	PVX	Chen et al. 2008
Hsp70cp-1 [a]	Upregulation	PVX	Chen et al. 2008
Hsp70er-1 [a]	Upregulation	PVX	Chen et al. 2008
Hsp90 [a]	ND	BaMV	Huang et al. 2012
Plastocyanin [a]	Not affected	PVX	Qiao et al. 2009
PsbO [a]	ND	PVX	Abbink et al. 2002
PsbO [a]	ND	AltMV	Lim et al. 2010
RabG3f [a]	Upregulation	BaMV	Huang et al. 2016
RabGAP1 [a]	Upregulation	BaMV	Huang et al. 2013
STKL [a]	Upregulation	BaMV	Cheng et al. 2013b
TIP [a]	ND	PVX	Fridborg et al. 2003
XRN4 [a]	Upregulation	BaMV	Lee et al. 2016

[a]: tobacco (*Nicotiana benthamiana*) gene

[b]: tomato (*Solanum lycopersicum*) gene

ND: Not discussed

doi:10.6342/NTU202003267

Table 2 Summary of preliminary transcriptome construction

Total Reads	190,142,562 reads
Mock reads	65,997,124 reads
CVX reads	58,861,704 reads
PiVX reads	65,283,734 reads
Paired reads	153,368,088 reads
Paired rate	80.7%
De novo assembly	60,510 contigs
Complete	9,557 contigs
Partial	10,744 contigs
Undefined	40,209 contigs
N_{50}	1,361 nt

doi:10.6342/NTU202003267

Table 3 List of pitaya primary targets

ContigID	BLAST ID	Gene description
PTY243	AT4G35090	Catalase 2 (*CAT2)*
PTY141	AT3G47470	Light-harvesting chlorophyll-protein complex I subunit A4 (*LHCA4*)
PTY189	AT1G79550	Phosphoglycerate kinase (*PGK*)
PTY898	AT1G61520	Photosystem I light harvesting complex gene 3 (*LHCA3*)
PTY1299	AT1G55670	Photosystem I subunit G (*PSAG*)
PTY961	AT1G30380	Photosystem I subunit K (*PSAK*)
PTY825	AT3G50820	Photosystem II subunit O-2 (*PSBO2*)
PTY642	AT3G50820	Photosystem II subunit O-2 (*PSBO2*)
PTY471	AT1G06680	Photosystem II subunit P-1 (*PSBP-1*)
PTY398	AT1G76100	Plastocyanin 1 (*PETE1*)
PTY607	AT3G16640	Translationally controlled tumor protein (*TCTP*)

doi:10.6342/NTU202003267

Table 4 Summary of full transcriptome construction

Total Reads	610,601,596 reads
Mock reads	197,056,782 reads
CVX reads	204,483,750 reads
PiVX reads	209,061,064 reads
Paired reads	340,735,552 reads
Paired rate	55.8%
De novo assembly	80,875 contigs
Complete	8,949 contigs
Partial	13,397 contigs
Undefined	58,529 contigs
N_{50}	1,377 nt

doi:10.6342/NTU202003267

Table 5 Genes presented in both CVX and PiVX infection network

Contig ID	BLAST ID	Gene description
ABA-related genes		
PTYV3_7455^{P}	AT5G51760.1	ABA-hypersensitive germination 1 (*AHG1*)
PTYV3_12070^{C}	AT3G11410.1	ABA-hypersensitive germination 3 (*AHG3*)
PTYV3_8051^{P}	AT1G60190.1	ARM repeat superfamily protein
PTYV3_15704^{C}	AT4G16563.1	Eukaryotic aspartyl protease family protein
PTYV3_18781^{C}	AT2G29380.1	Highly ABA-induced PP2C gene 3 (*HIA3*)
PTYV3_10703^{P}	AT2G26190.1	Calmodulin-binding family protein (*IQM4.1*)
PTYV3_16402^{P}	AT2G26190.1	Calmodulin-binding family protein (*IQM4.2*)
PTYV3_180^{P}	AT3G21670.1	NRT1/PTR family 6.4 (*NPF6.4.2*)
PTYV3_6682^{P}	AT2G47770.1	Outer membrane tryptophan-rich sensory protein-related (*TSPO.1*)
PTYV3_6685^{P}	AT2G47770.1	Outer membrane tryptophan-rich sensory protein-related (*TSPO.2*)
Auxin-related genes		
PTYV3_5908^{C}	AT1G68050.1	Flavin-binding, kelch repeat, f box 1 (FKF1/ADO3)
PTYV3_3930^{P}	AT3G56370.1	Leucine-rich repeat protein kinase family protein (*IRK.1*)
BR-related gene		
PTYV3_2787^{C}	AT4G08950.1	Exordium (*EXO.1*)
Chloroplast-related gene		
PTYV3_658^{C}	AT3G47080.1	Tetratricopeptide repeat (TPR)-like superfamily protein

doi:10.6342/NTU202003267

Ethylene-related gene		
PTYV3_1126[P]	AT1G77330.1	ACC Oxidase 5 (*ACO5*)
General stress-related genes		
PTYV3_3287[P]	AT1G77380.1	Amino acid permease 3 (*AAP3*)
PTYV3_2281[P]	AT2G30020.1	Protein phosphatase 2C family protein (*AP2C1*)
PTYV3_15506[C]	AT1G01490.1	Heavy metal transport/detoxification superfamily protein (*HIPP39*)
PTYV3_13478[P]	AT2G26150.1	heat shock transcription factor A2 (*HSFA2.2*)
PTYV3_18066[P]	AT1G25450.1	3-ketoacyl-CoA synthase 5 (*KCS5*)
PTYV3_23428[P]	AT3G09040.1	Mitochondrial rna editing factor 12 (*MEF12*)
PTYV3_15872[P]	AT3G47640.1	Popeye (*PYE*)
PTYV3_22670[C]	AT5G59820.1	Responsive to high light 41 (*RHL41*/*ZAT12*)
PTYV3_14897[P]	AT3G18950.1	Transducin/WD40 repeat-like superfamily protein
GA-related gene		
PTYV3_5416[C]	AT4G17230.1	SCARECROW-like 13 (*SCL13*)
JA-related gene		
PTYV3_2088[P]	AT1G17420.1	Lipoxygenase 3 (*LOX3.1*)
Multiple hormone-related genes		
PTYV3_11620[P]	AT1G01480.1	1-amino-cyclopropane-1-carboxylate synthase 2 (*ACC2*/*ASC2*)
PTYV3_19113[P]	AT4G17615.1	Calcineurin B-like protein 1 (*CBL1*)
PTYV3_6934[C]	AT4G20780.1	Calmodulin like 42 (*CML42*)

doi:10.6342/NTU202003267

PTYV3_27093[P]	AT4G27410.3	NAC (No Apical Meristem) domain transcriptional regulator superfamily protein (*RD26*/*ANAC72*)
PTYV3_6261[P]	AT2G38470.1	WRKY DNA-binding protein 33 (*WRKY33*)
PTYV3_10665[P]	AT1G80840.1	WRKY DNA-binding protein 40 (*WRKY40*)
Non-classified genes		
PTYV3_6809[P]	AT5G09220.1	Amino acid permease 2 (*AAP2*)
PTYV3_21544[P]	AT1G61820.1	Beta glucosidase 46 (*BGLU46*)
PTYV3_66[C]	AT1G61800.1	Glucose-6-phosphate/phosphate translocator 2 (*GPT2*)
PTYV3_11365[P]	AT1G13390.1	Translocase subunit secA
PTYV3_2799[C]	AT2G34470.2	Urease accessory protein G (*UREG*/*PKSF109*)
ROS-related gene		
PTYV3_21350[C]	AT1G09530.1	Phytochrome interacting factor 3 (*PIF3*) [R]

[C]: complete gene

[P]: partial gene

doi:10.6342/NTU202003267

Supplementary data

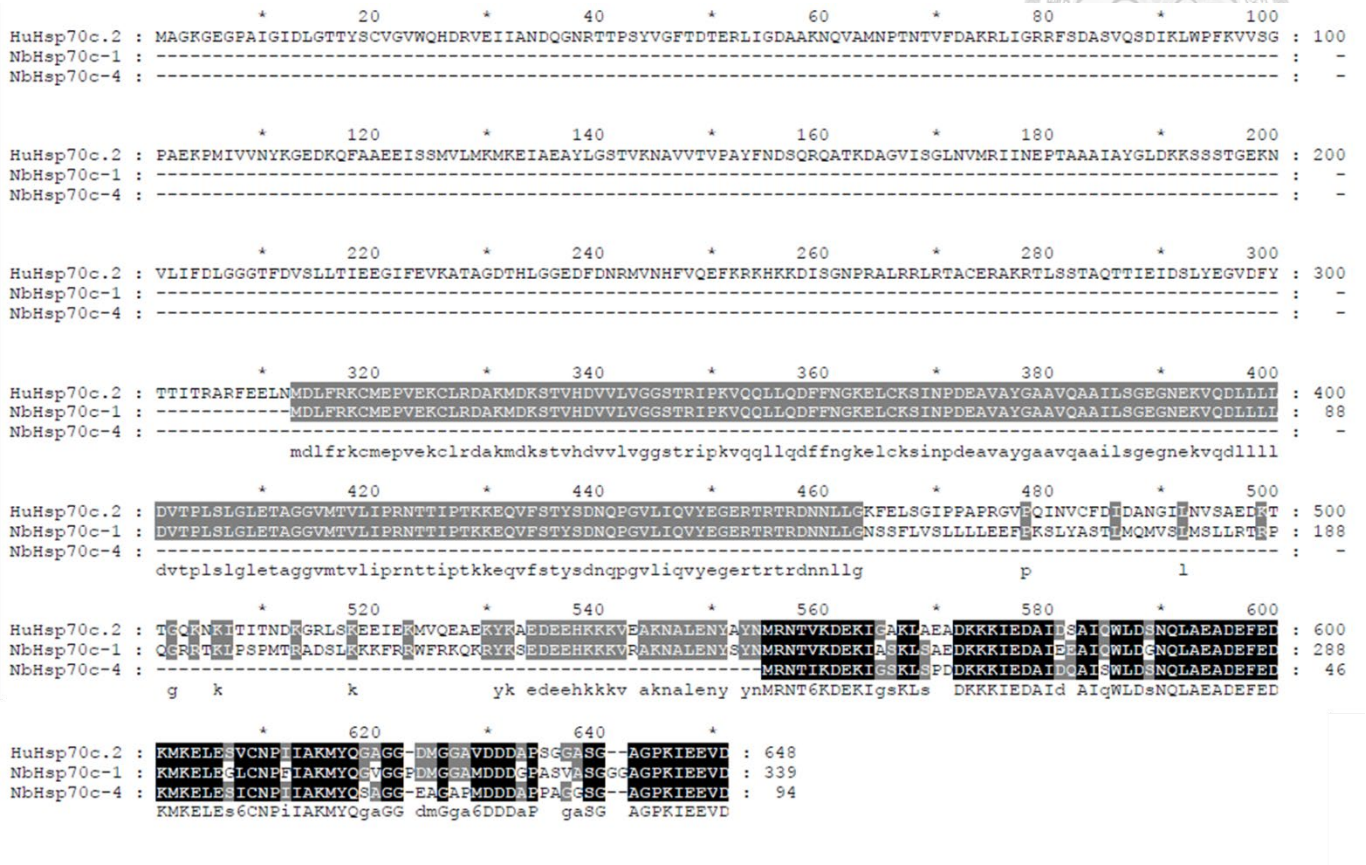

Fig. S1 Amino acid alignment of Hsp70c-1, Hsp70c-4, and HuHsp70c.2 (PTYV3_1546)

doi:10.6342/NTU202003267

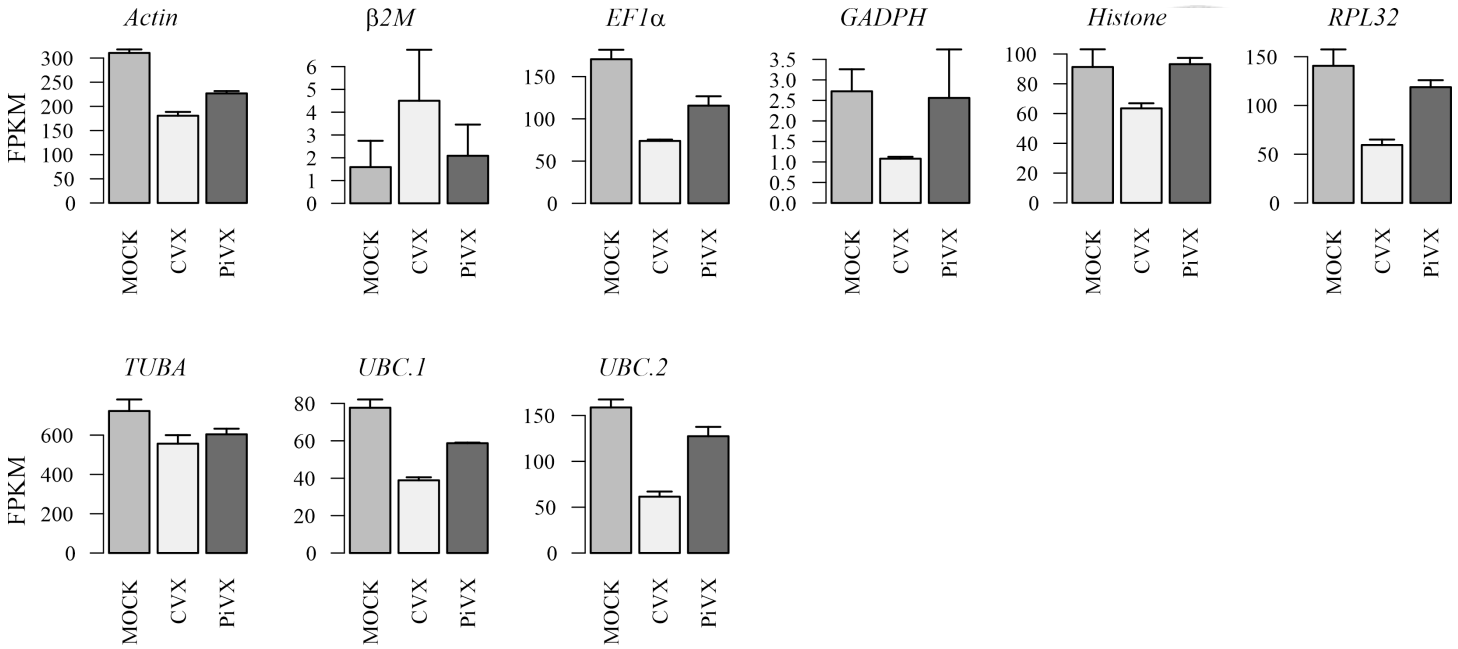

Fig. S2 Expression levels of potential reference genes for pitaya.

Expression levels of these genes are shown as FPKM with SE value calculated.

doi:10.6342/NTU202003267

Table S1 Primers used in this study

qRT-PCR primers		
HuATHSPRO2-F1	GGGAAGCCCAATCTCGACTA	This study
HuATHSPRO2-R1	TTGCCTGCGTAGATCCATGA	This study
HuPSAK-F1	AGGCAAAGGCAAAGGGAAAG	This study
HuPSAK-R1	CGGCAAACAACATCAGGGTA	This study
HuPSAO-F1	TTGTACCTTTCCGAGGGATT	This study
HuPSAO-R1	GTGAGGCTGTTTCCATTGAT	This study
HuLHCB2.1-F1	ACCTTGGTAACCCGAACCTT	This study
HuLHCB2.1-R1	CCCGGAAACTCTGTAACCCT	This study
HuDI21-F1	TCAGGAAGAGATGGCGAAGG	This study
HuDI21-R1	TTCAGCGACGTCGATCTCAT	This study
HuPGK-F1	CGTGGCAAACCCAAAGAAAC	This study
HuPGK-R1	CTCCACAAGAGAGGAACCCA	This study
HuPETE1-F1	ATCGCCATCTCCTCCTTCAC	This study
HuPETE1-R1	GCGACACCAAAGTCCTTCAG	This study
HuPSAG-F1	CCATGGTCTCACCAAACCAG	This study
HuPSAG-R1	GCACCTGCTTGGCTACATTC	This study
HuGRP7-F3	CATCAACGACCGTGAGACTG	This study
HuGRP7-R4	CACCAGATCCACGAGATTGA	This study

doi:10.6342/NTU202003267

semi-qRT-PCR primers		
NbHSp70c-1F	AAGAGCATCAACCCTGATGAG	This study
NbHsp70c-1R	TTGGATGGCTTCCTCAATGGCA	This study
Hsp70c-4F	GGATGATAAGATTAGTTCTAAGC	(Chen et al.,2008)
Hsp70c-4R	CACACTTAATCGACCTCC	(Chen et al.,2008)
Hsp70er-1F	GTCAAGGCTAATTTACATTTC	(Chen et al.,2008)
Hsp70er-1R	GCAGCAAGTTCTTTATGTCTG	(Chen et al.,2008)
Hsp70cp-1F	GTGGAGTCATGACCAAAATTATC	(Chen et al.,2008)
Hsp70cp-1R	GAAGTCTGCATCGATAAC	(Chen et al.,2008)
NbRbcsF	CCTCTGCAGTTGCCACC	(Chen et al.,2008)
NbRbcSR	CCTGTGGGTATGCCTTCTTC	(Chen et al.,2008)

doi:10.6342/NTU202003267